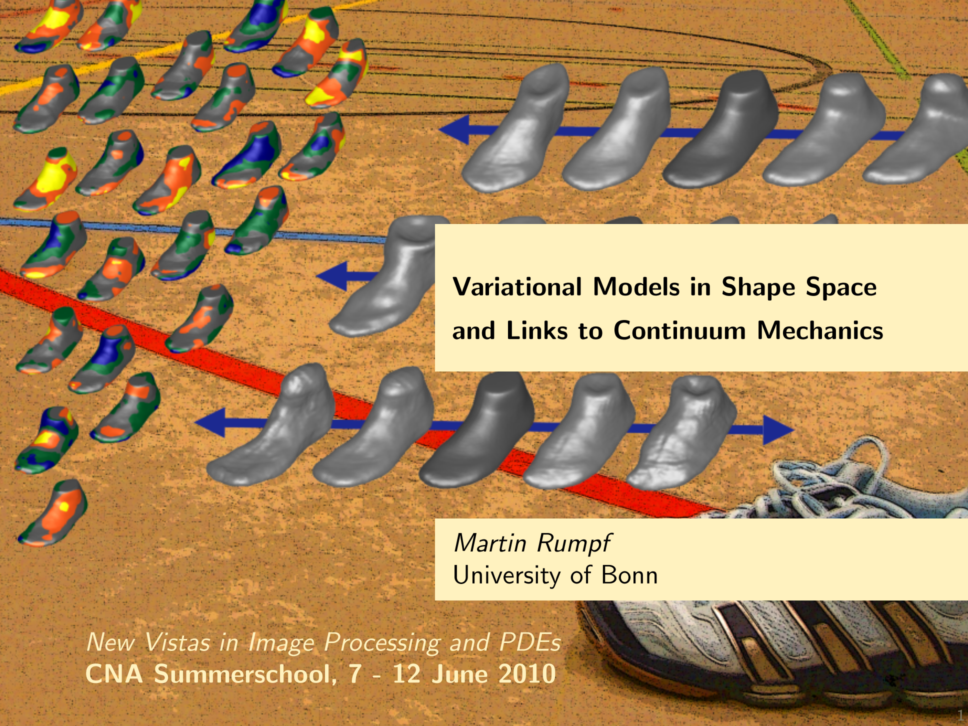

Variational Models in Shape Space and Links to Continuum Mechanics

Martin Rumpf
University of Bonn

New Vistas in Image Processing and PDEs
CNA Summerschool, 7 - 12 June 2010

joint work with

- Benedikt Wirth (Bonn)
- Leah Bar (Minneapolis)
- Guillermo Sapiro (Minneapolis)

Overview

- A Teaser
- Two different shape space concepts
- A brief review of some related work
- Elasticity-based shape averaging
- Elasticity-based shape PCA
- Viscous fluid based shape space
- Conclusions
- Recommended reading

Extended abstract

The analysis of shapes as elements in a frequently infinite-dimensional space of shapes has attracted increasing attention over the last decade. There are pioneering contributions in the theoretical foundation of shape space as a Riemannian manifold as well as path-breaking applications to quantitative shape comparison, shape recognition, and shape statistics. The aim of this lecture series is to adopt a primarily physical perspective on the space of shapes and to relate this to the prevailing geometric perspective. Indeed, we here consider shapes given as boundary contours of volumetric objects, which consist either of an elastic solid or a viscous fluid.

Extended abstract (cont)

In the first case, shapes are transformed via elastic deformations, where the associated elastic energy only depends on the final *state* of the deformation and not on the path along which the deformation is generated. The minimal elastic energy required to deform an object into another one can be considered as a dissimilarity measure between the corresponding shapes. We apply this approach for shape averaging and shape statistics. Thereby, an elastic deformation is assigned to each shape. The shape average is then described as the common image under all elastic deformations of the given shapes, which minimizes the total elastic energy stored in these deformations. The model is relaxed involving a further energy which measures how well the elastic deformation image of a particular shape matches the average shape, and a suitable shape prior can be considered for the shape average. Shapes are represented via their edge sets, which also allows for an application to averaging image morphologies described via ensembles of edge sets. Furthermore, based on the notion of nonlinear elastic deformations from one shape to another, a suitable linearization of geometric shape variations is introduced.

Extended abstract (cont)

Furthermore, a covariance metric — an inner product on linearized shape variations — is introduced, which robustly captures strongly nonlinear geometric variations in a physically meaningful way and allows to extract the dominant modes of shape variation. Here, we compare a standard L^2-type covariance metric with a metric based on the Hessian of the nonlinear elastic energy. To make this approach computationally tractable, in this case sharp edges are approximated via phase fields, and a corresponding variational phase field model is derived. Finite elements are applied for the spatial discretization, and a multi-scale alternating minimization approach allows the efficient computation of shape averages in 2D and 3D.

Extended abstract (cont)

In the second case, shapes are transformed into each other via viscous transport of fluid material, and the flow naturally generates a connecting *path* in the space of shapes. The viscous dissipation rate—the rate at which energy is converted into heat due to friction—can be defined as a metric on an associated Riemannian manifold. Hence, via the extraction of shortest transport paths one defines a distance measure between shapes. The approach can easily be generalized to shapes given as segment contours of multi-labeled images and to geodesic paths between partially occluded objects. The proposed computational framework for finding such a minimizer is based on the time discretization of a geodesic path as a sequence of pairwise matching problems, which is strictly invariant with respect to rigid body motions and ensures a 1-1 correspondence along the induced flow in shape space. When decreasing the time step size, the model leads to the minimization of the actual geodesic length, where the Hessian of the pairwise matching energy reflects the chosen Riemannian metric on the underlying shape space.

Extended abstract (cont)

If the constraint of pairwise shape correspondence is replaced by the volume of the shape mismatch as a penalty functional, one obtains for decreasing time step size an optical flow term controlling the transport of the shape by the underlying motion field. The method is implemented via a level set representation of shapes, and a finite element approximation is again employed as spatial discretization both for the pairwise matching deformations and for the level set representations.

Beyond a detailed presentation of these two approaches we give a detailed comparison of the *path*-based and the *state*-based approach. This lecture series is based on joint work with Leah Bar, Guillermo Sapiro from the University of Minnesota at Minneapolis and Benedikt Wirth from the University of Bonn.

Average of 3D kidneys

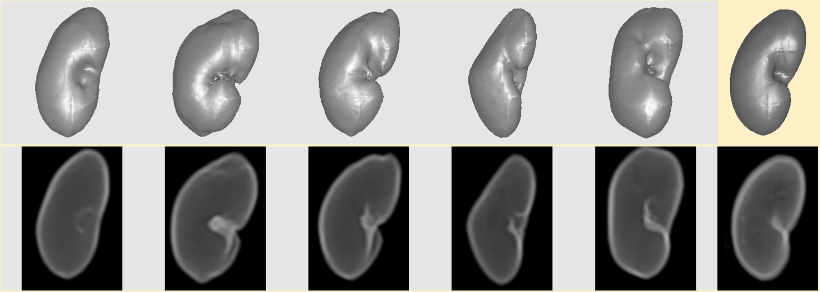

Five kidneys and their average (right).

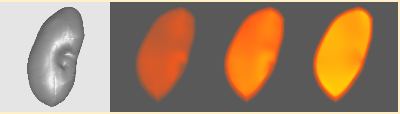

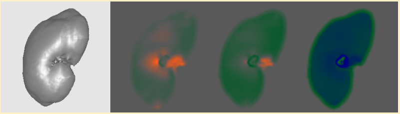

- A Teaser
- **Shape PCA for scanned 3D feet**

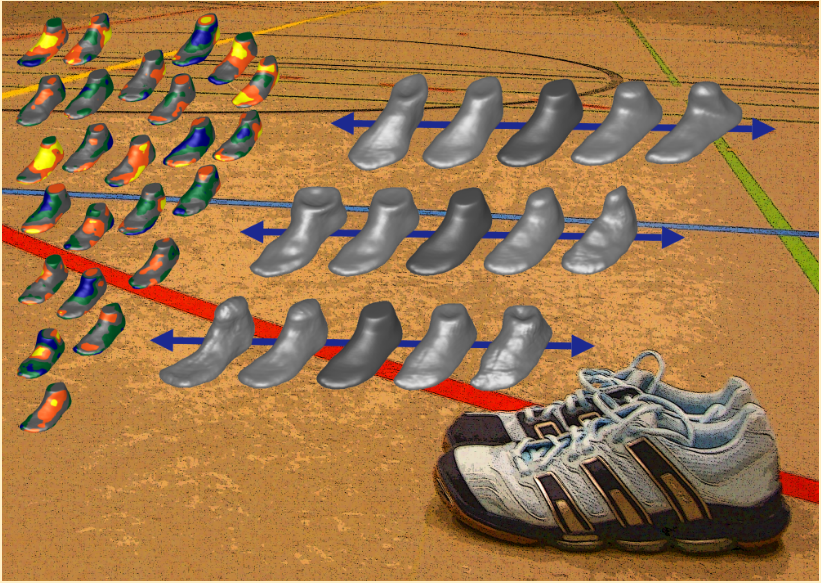

Nonlinear interpolation in multi–component cell motion

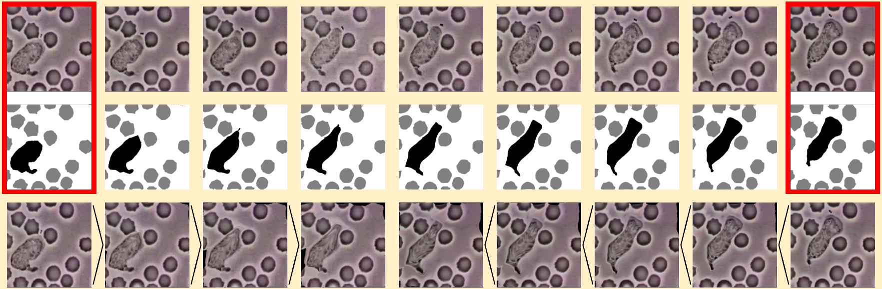

Two different concepts

- Recalling the finite dimensional case
- Path based Riemannian setup
- State based elastic approach

- Recalling the finite dimensional case
- Path based Riemannian setup
- State based elastic approach

Some simple physics:

Geodesic distance between $x_1, x_2 \in \mathbb{R}^d$ is $\|x_2 - x_1\|_2$.

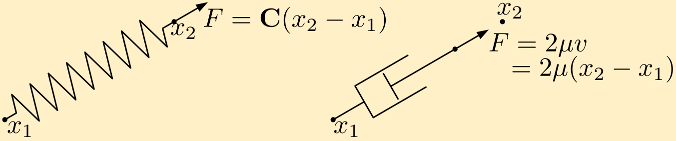

- **Spring model:** By Hooke's law—the elastic energy of a spring extended from x_1 to x_2 is $\mathcal{W} = \frac{1}{2}\mathbf{C}\|x_2 - x_1\|_2^2 \longrightarrow$ state based
- **Dashpot model:** The dissipated energy of a dashpot which is extended from x_1 to x_2 at constant speed is $\mathbf{Diss} = \int_0^1 2\mu\|v\|_2^2 \,\mathrm{d}t = 2\mu\|x_2 - x_1\|_2^2 \longrightarrow$ path based

Using this physical interpretation, we can express for instance the arithmetic mean $x = \frac{1}{n}\sum_{i=1}^n x_i = \operatorname{argmin}_{\tilde{x}} \sum_{i=1}^n \|x_i - \tilde{x}\|_2^2$ either as the minimizer of the total elastic deformation energy $\mathcal{W}$ in a system where x is connected to each x_i by elastic springs or as the minimizer of the total viscous dissipation when extending dashpots from x_i to x.

- A Riemannian manifold is a set $\mathcal{M}$ that is locally diffeomorphic to Euclidean space.
- Given a path $x(t) \in \mathcal{M}$, $t \in [0,1]$, we define its derivative $\dot{x}(t)$ as a tangent vector to $\mathcal{M}$ at $x(t) \longrightarrow T_{x(t)}\mathcal{M}$
- $T_{x(t)}\mathcal{M}$ is equipped with the metric $g_{x(t)}(\cdot,\cdot)$
- The length of a path $x(t) \in \mathcal{M}$, $t \in [0,1]$, is defined as $\int_0^1 \sqrt{g_{x(t)}(\dot{x}(t),\dot{x}(t))}\,\mathrm{d}t$, and locally shortest paths are denoted geodesics.
- There is a bijection $\exp_x : T_x\mathcal{M} \to \mathcal{M}$ of a neighborhood of $0 \in T_x\mathcal{M}$ into a neighborhood of $x \in \mathcal{M}$ that assigns to each tangent vector $v \in T_x\mathcal{M}$ the end point of the geodesic emanating from x with initial velocity v.

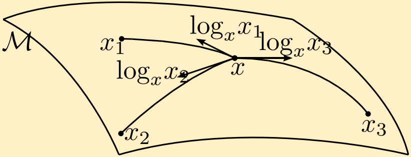

$\longrightarrow$ enables the definition mean and PCA later.

In a Riemannian space $\mathcal{M}$, the path-based approach directly applies:

$\int_0^1 g_{x(t)}(\dot{x}(t), \dot{x}(t))\,\mathrm{d}t$ can be considered as the energy dissipation $\mathbf{Diss}$ spent to move a point from $x(0)$ to $x(1)$ along a geodesic.

Why is this consistent with geodesics on a finite dimensional manifold?

Let $\mathcal{M}$ be a finite dimensional Riemannian manifold and consider a curve $s : [0,1] \to \mathcal{M}$ with $s(0) = s_A$ and $s(1) = s_B$, then s is a (shortest) geodesic connecting s_A and s_B, iff

$$\int_0^1 \sqrt{g(\dot{s},\dot{s})}\,\mathrm{d}t \leq \int_0^1 \sqrt{g(\dot{c},\dot{c})}\,\mathrm{d}t$$

$\Leftrightarrow$

$$\int_0^1 g(\dot{s},\dot{s})\,\mathrm{d}t \leq \int_0^1 g(\dot{c},\dot{c})\,\mathrm{d}t$$

for all curves $c : [0,1] \to \mathcal{M}$ with $c(0) = s_A$ and $c(1) = s_B$.

For any reasonable (even finite-dimensional) model of shape space, objects are not rigid, and the inner relation between points defines the **Riemannian** (and thus the **path-based**) structure:

- Dissipation $\mathbf{Diss}$ reflects the internal interaction accumulated in time.
- This dissipation depends significantly on the path in shape space.

In contrast, when applying the **state-based approach**:

- we directly compare the state of internal interaction independent of time
- i.e. there is no history of these relations
- This comparison can be quantified based on a stored (elastic) interaction energy: $\sqrt{\mathcal{W}}$.
- which is then a quantitative measure of the dissimilarity of the two objects but in general no metric distance.

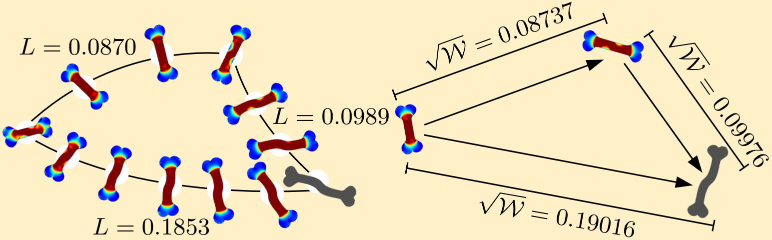
$L = 0.0870$
$L = 0.0989$
$L = 0.1853$
$\sqrt{\mathcal{W}} = 0.08737$
$\sqrt{\mathcal{W}} = 0.09976$
$\sqrt{\mathcal{W}} = 0.19016$

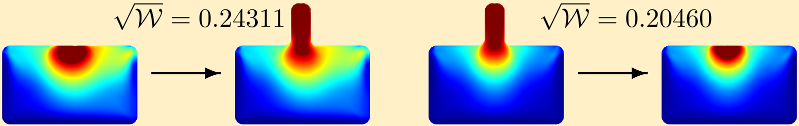
$\sqrt{\mathcal{W}} = 0.24311$
$\sqrt{\mathcal{W}} = 0.20460$

Two different concepts ≫

- Recalling the finite dimensional case
- Path based Riemannian setup
- State based elastic approach

Viscosity describes the internal resistance in a fluid as a macroscopic measure of the friction between fluid particles.

(viscosity of honey is significantly larger than that of water)

Mathematically, the friction is described in terms of the (symmetric) stress tensor

$$\sigma = (\sigma_{ij})_{ij=1,\dots d}$$

whose entries represent a force per area element. (σ_{ij} is the force in x_i direction acting on an area element normal to the x_j direction)

In a (monopolar) fluid: $\sigma = \sigma(\mathcal{D}v)$ (v velocity)

$$\mathcal{D}v := (\tfrac{\partial v_i}{\partial x_j})_{ij=1,\dots d}$$

A short review of dissipation in continuum mechanics (cont)

For rigid body motions the stress should vanish:

rotational component of the local motion is $\frac{1}{2}(\mathcal{D}v - (\mathcal{D}v)^T)$
(local rotation axis $\nabla \times v$ and angular velocity $|\nabla \times v|$)

$\longrightarrow \sigma = \sigma(\epsilon[v])$ with $\epsilon[v] := \frac{1}{2}(\mathcal{D}v + (\mathcal{D}v)^T)$

compressive stresses	$\leftrightarrow$	$\mathrm{tr}(\mathcal{D}v)$ (trace of $\mathcal{D}v$)
shear stresses	$\leftrightarrow$	trace-free part of $\mathcal{D}v$

$$
\begin{aligned}
\sigma_{ij} &= \mu\,(\sigma_{\text{shear}})_{ij} + K_c\,(\sigma_{\text{bulk}})_{ij} \\
&:= \mu\left(\frac{\partial v_i}{\partial x_j} + \frac{\partial v_j}{\partial x_i} - \frac{2}{d}\sum_k \frac{\partial v_k}{\partial x_k}\delta_{ij}\right) + K_c \sum_k \frac{\partial v_k}{\partial x_k}\delta_{ij} \\
&= \lambda\delta_{ij}\mathrm{tr}(\epsilon[v]) + 2\mu\epsilon_{ij}[v]
\end{aligned}
$$

(μ viscosity, K_c modulus of compression, $\lambda := K_c - \frac{2\mu}{d}$)

A short review of dissipation in continuum mechanics (cont)

a simple example:

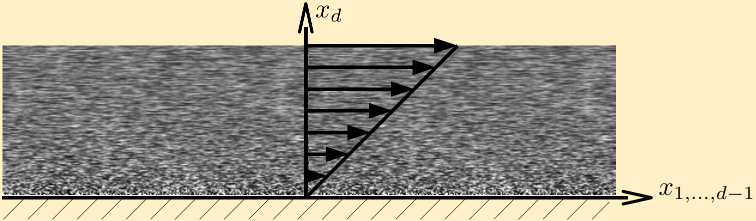

$$v(x) = \frac{x_d}{H} v^\partial \qquad \longrightarrow$$

pure shear stress $\mu \frac{v^\partial}{H}$ on horizontal area elements

A short review of dissipation in continuum mechanics (cont)

local rate of viscous dissipation: the rate at which mechanical energy is locally converted into heat due to friction

$$\mathbf{diss}[v] = \frac{\lambda}{2}(\mathrm{tr}\epsilon[v])^2 + \mu \mathrm{tr}(\epsilon[v]^2)\,,$$

indeed σ is the first variation of the local dissipation rate:

$$\delta_{(Dv)_{ij}}\mathbf{diss} = \lambda\,\mathrm{tr}\epsilon\,\delta_{ij} + 2\mu\,\epsilon_{ij} = \sigma_{ij}$$

accumulated global dissipation of the motion field v in the time interval $[0,1]$ on a path of a moving object $(\mathcal{O}(t))_{t\in[0,1]}$:

$$\mathbf{Diss}\left[(v(t),\mathcal{O}(t))_{t\in[0,1]}\right] = \int_0^1\int_{\mathcal{O}(t)}\mathbf{diss}[v]\,\mathrm{d}x\,\mathrm{d}t$$

- A metric $\mathcal{G}$ on the (infinite-dimensional) manifold $\mathbf{S}$ assigns each element $\mathcal{S} \in \mathbf{S}$ an inner product on variations $\delta\mathcal{S}$ of $\mathcal{S}$.
- The length of a differentiable curve $\mathcal{S} : [0,1] \to \mathbf{S}$ is then given by $L[\mathcal{S}] = \int_0^1 \|\dot{\mathcal{S}}(t)\| \,\mathrm{d}t = \int_0^1 \sqrt{\mathcal{G}[\mathcal{S}(t)](\dot{\mathcal{S}}(t), \dot{\mathcal{S}}(t))} \,\mathrm{d}t.$
- An infinitesimal variation $\delta\mathcal{S}$ of a shape $\mathcal{S} = \partial\mathcal{O}$ is associated with a (non–unique) transport field $v \in \mathcal{V}(\delta\mathcal{S})$:

$$v(x) \cdot \nu[\mathcal{S}](x) = \delta\mathcal{S}(x) \cdot \nu[\mathcal{S}](x) \text{ for all } x \in \mathcal{S}$$

- The metric in terms of the motion field:

$$\mathcal{G}(\delta S, \delta S) := \min_{v \in \mathcal{V}(\delta\mathcal{S})} \int_{\mathcal{O}} \mathbf{diss}[v] \,\mathrm{d}x$$

2.1 Definition (Geodesic path). *A geodesic path between $\mathcal{S}_A$ and $\mathcal{S}_B$ in $\mathbf{S}$ is a curve $(\mathcal{S}(t))_{t\in[0,1]} \subset \mathbf{S}$ with $\mathcal{S}(0) = \mathcal{S}_A$ and $\mathcal{S}(1) = \mathcal{S}_B$ which is a local minimizer of*

$$\min_{v(t)\in\mathcal{V}(\dot{\mathcal{S}}(t))} \mathbf{Diss}\left[(v(t), \mathcal{O}(t))_{t\in[0,1]}\right]$$

among all differentiable paths in $\mathbf{S}$.

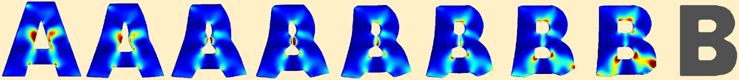

geodesic path ($L = 0.2225$, $\mathbf{Diss} = 0.0497$)

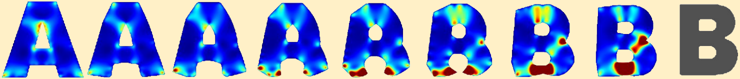

non geodesic path ($L = 0.2886$, $\mathbf{Diss} = 0.0880$)

computation based on a variational time discretization

Two different concepts ≫

- Recalling the finite dimensional case
- Path based Riemannian setup
- State based elastic approach

Deformation of length, area and volume:

- $|\mathcal{D}\phi| = \sqrt{\mathrm{tr}(\mathcal{D}\phi^T\mathcal{D}\phi)}$ controls the averaged change of length:

$$\int_0^1 |\frac{\mathrm{d}}{\mathrm{d}t}(\phi\circ c)(t)|\,\mathrm{d}t = \int_0^1 \sqrt{\mathcal{D}\phi\,\dot{c}\cdot\mathcal{D}\phi\,\dot{c}}\,\mathrm{d}t = \int_0^1 \sqrt{\mathcal{D}\phi^T\mathcal{D}\phi\,\dot{c}\cdot\dot{c}}\,\mathrm{d}t$$

- $|\mathrm{cof}\mathcal{D}\phi|$ controls the averaged change of area:

$$\nu^\phi = |\mathrm{cof}\mathcal{D}\phi\,\nu|^{-1}\mathrm{cof}\mathcal{D}\phi\,\nu\,,\quad \mathsf{d}a^\phi = |\mathrm{cof}\mathcal{D}\phi\,\nu|\,\mathsf{d}a$$

  where $\mathrm{cof}\,A = \det A\; A^{-T}$.

- $|\det\mathcal{D}\phi|$ controls the local change of volume

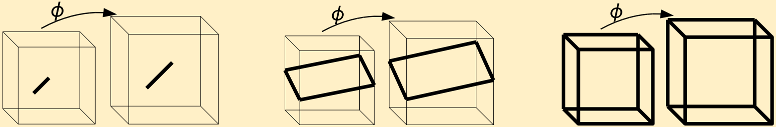

$|\mathrm{D}\phi|$ length variation　　$|\mathrm{cof}(\mathrm{D}\phi)|$ area variation　　$\det(\mathrm{D}\phi)$ volume variation

- **Cauchy stress tensor:** $\sigma^\phi = (\sigma^\phi_{ij})_{ij}$ in deformed config.
- Transformation of force density:

  $\sigma\,\nu\,\mathrm{d}a = \sigma^\phi \nu^\phi\,\mathrm{d}a^\phi \Rightarrow \sigma = \sigma^\phi \mathrm{cof}\mathcal{D}\phi$
- **Axiom of elasticity:** $\sigma = \sigma(\mathcal{D}\phi)$
- **Hyperelasticity:**

  stored elastic energy: $\mathcal{W}[\phi] = \int_\Omega W(\mathcal{D}\phi)\,\mathrm{d}x$

  Euler Lagrange equations: $\int_\Omega W_{,A}(\mathcal{D}\phi) : \mathcal{D}\psi\,\mathrm{d}x = 0$

  $\longrightarrow -\mathrm{div}\, W_{,A}(\mathcal{D}\phi) = 0$ in $\Omega\,,\;\; W_{,A}(\mathcal{D}\phi)\nu = 0$ on $\partial\Omega$.

  Relating stress and energy: $\sigma = W_{,A}$
- **frame indifference**: $W(\mathcal{D}\phi) = \tilde{W}(\mathcal{D}\phi^T\mathcal{D}\phi)$
- **isotropy**: $W(\mathcal{D}\phi) = \bar{W}(I_1, I_2, I_3)$ where
  I_1, I_2, I_3 are the principal invariance of $\mathcal{D}\phi^T\mathcal{D}\phi$:
  $I_1 = |\mathcal{D}\phi|^2$, $I_2 = |\mathrm{cof}\mathcal{D}\phi|^2$, $I_3 = \det\mathcal{D}\phi$

A short review of elasticity (cont.)

- we consider a slightly more general:

$$W(A) = \hat{W}(A, \mathrm{cof}A, \det A)$$

and later assume that $\hat{W}$ is convex.

- **Linearized elasticity:**

$$\mathcal{W}^{lin} = \int_\Omega \frac{\lambda}{2}(\mathrm{tr}\epsilon[u])^2 + \mu\mathrm{tr}(\epsilon[u]^2)\,\mathrm{d}x$$

where $\epsilon[u] = \frac{1}{2}(\mathcal{D}u + \mathcal{D}u^T)$

drawbacks:

rigid body motion invariant only for infinitesimal displacements

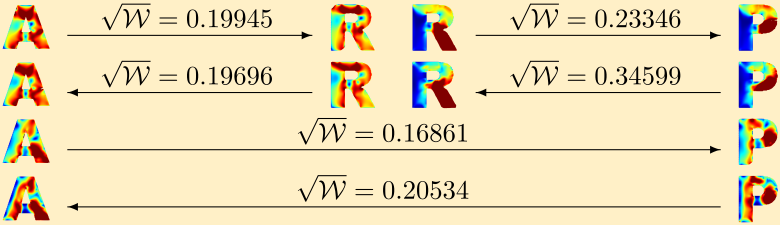

Dissimilarity measure between two different shapes:

$$d_{\mathsf{elast}}(\mathcal{S}_A, \mathcal{S}_B) := \min_{\phi, \phi(\mathcal{S}_A) = \mathcal{S}_B} \sqrt{\mathcal{W}[\phi, \mathcal{O}_A]}\,.$$

The very first appearance of the notion shape space

David G. Kendall: Shape manifolds, procrustean metrics, and complex projective spaces. 1984

- Polygons with vertices $P_1, P_2, \ldots, P_k$ in $\mathbb{R}^m$
- Define Shape space as the quotient space

$$\Sigma_m^k = \{(\mathbb{R}^m)^{k-1} \setminus 0\}/\mathsf{Sim}\,,$$

where Sim denotes the group of similarities generated by the rotations and dilatations

G. Charpiat, O. Faugeras, R Keriven: Approximations of Shape Metrics and Applications to Shape Warping and Empirical Shape Statistics, 2005

- distance measure between closed sets

$$\rho(\Omega_1, \Omega_2) = \sup_{x \in D} |d_{\Omega_1}(x) - d_{\Omega_2}(x)|$$

- equivalent to the Hausdorff-metric

$$\rho_H(\Omega_1, \Omega_2) = \max \left\{ \sup_{x \in D} d_{\Omega_1}(x), \sup_{x \in D} d_{\Omega_2}(x) \right\}$$

- implemented via an approximations based on

$$\sup_{x' \in \Gamma'} d_{\Gamma}(x') = \lim_{\beta \to +\infty} \left(\frac{1}{|\Gamma'|} \int_{\Gamma'} d_{\Gamma}^{\beta}(x') d\Gamma'(x') \right)^{1/\beta}$$

F. Mémoli, G. Sapiro: A Theoretical and computational framework for isometry invariant recognition of point cloud data,

Consider bounded metric spaces (X, d_X) and (Y, d_Y).

Then the **Gromov-Hausdorff distance** $d_{GH}(,)$ is given by

$$d_{GH}(X,Y) = \inf_{\substack{\phi:X\to Y \\ \psi:Y\to X}} \sup_{\substack{x_1,x_2\in X \\ y_1,y_2\in Y \\ (x_i,y_i)\in G(\phi,\psi)}} |d_X(x_1,x_2) - d_Y(y_1,y_2)|$$

where $G(\phi,\psi) = \{(x,\phi(x)), x \in X\} \cup \{(\psi(y),y), y \in Y\}$ and the infimum is taken over all arbitrary maps $\phi : X \to Y$ and $\psi : Y \to X$.

in case of point clouds:

for discrete metric spaces $(\mathbb{X} = \{x_1,\ldots,x_n\}, d_{\mathbb{X}})$ and $(\mathbb{Y} = \{y_1,\ldots,y_n\}, d_{\mathbb{Y}})$ we define

$$d(\mathbb{X},\mathbb{Y}) = \min_{\pi\in\Pi_n} \max_{1\leq i,j\leq n} |d_{\mathbb{X}}(x_i,x_j) - d_{\mathbb{Y}}(y_{\pi_i},y_{\pi_j})|$$

G. Charpiat, O. Faugeras, R Keriven (see above)

Empirical mean (E based on Hausdorff distance and perimeter):

$$\frac{1}{N}\sum_{i=1,\ldots,N} E^2(\Gamma,\Gamma_i) \longrightarrow \min$$

Empirical covariance

- gradient of $\Gamma \to E^2(\Gamma,\Gamma_i)$ defines a normal velocity field β_i
- consider infinitesimal deformation $x - \varepsilon\beta_i(x)\mathbf{n}(x)$ of Γ
- mean velocity $\bar{\beta} = (1/N)\sum_{i=1}^{N}\beta_i$
- define the covariance operator $\Lambda : L^2(\Gamma) \to L^2(\Gamma)$ such that

$$\beta \to \sum_{i=1}^{N} g(\beta,(\beta_i-\bar{\beta}))(\beta_i-\bar{\beta})$$

P. T. Fletcher, S. Venkatasubramanian, S. Joshi: Robust statistics on Riemannian manifolds via the geometric median. 2008

- Let M be a Riemannian manifold. The weighted geometric median is defined as

$$m = \mathrm{argmin}_{x \in M} \sum_{i}^{N} w_i d(x, x_i)$$

- iterative scheme to compute the geometric median:

$$\begin{aligned} m_{k+1} &= m_k - \alpha G_k \\ G_k &= \sum_{i \in I_k} \frac{w_i x_i}{d(x_i, m_k)} \cdot \Big(\sum_{i \in I_k} \frac{w_i}{d(x_i, m_k)} \Big)^{-1} \end{aligned}$$

M. Kilian, N. J. Mitra, H. Pottmann:
Geometric modeling in shape space, 2007

- triangular meshes $\mathcal{S}$ are treated as shapes in a shape space
- the tangent bundle of $\mathcal{S}$ is given by discrete vector fields
- a deformation field at time t is given by

$$X(t) := \Big(\frac{d}{dt}p(t)\Big)_{p \text{ nodes of } \mathcal{S}}$$

- definition of the **Riemannian metric**

$$G(X,Y) := \sum_{p,q \text{ nodes of } \mathcal{S}} (X_p - X_q) \cdot (p-q)\,(Y_p - Y_q) \cdot (p-q)$$

where $X_p \in \mathbb{R}^3$ for each tangent vector X.

F. R. Schmidt, M. Clausen, D. Cremers: Shape matching by variational computation of geodesics on a manifold, 2006

manifold of preshapes:

- closed planar curves c parametrized over $\mathbb{S}^1$ and represented by the velocity c' instead of the curve c itself
- *arclength* parametrization: $c'(e^{it}) = e^{i\vartheta(t)}$, where $\vartheta : [0, 2\pi] \to \mathbb{R}$
- **shape space** $\mathbf{S}$ consists of all orbits $\vartheta \cdot \mathbb{S}^1$

geodesic distance between two shapes $\vartheta_1 \cdot \mathbb{S}_1^1$ and $\vartheta_2 \cdot \mathbb{S}_2^1$:

$$\inf_{s_1 \in \mathbb{S}_1^1} \inf_{s_2 \in \mathbb{S}_2^1} \|\vartheta_1 \cdot s_1 - \vartheta_2 \cdot s_2\|_{L^2} = \inf_{s \in \mathbb{S}^1} \|\vartheta_1 - \vartheta_2 \cdot s\|_{L^2}$$

P. W. Michor, D. Mumford:
Riemannian geometries on spaces of plane curves, 2005

- space of smooth regular curves in the plane viewed as the orbit space of maps on $\mathbb{S}^1$ modulo reparameterizations
- **Riemannian metric:**

$$g_c^A(v,w) := \int_{\mathbb{S}^1} (1 + A\kappa_c(\theta)^2)\langle v(\theta), w(\theta)\rangle |c'(\theta)| d\theta$$

  where κ_c is the curvature of the curve c and v, w are normal vector fields to c
- $A\kappa_c^2$ is a regularization term:
  for $A = 0$ the geodesic distance between two distinct curves is 0, while for $A > 0$ the distance is always positive
- interesting properties of the space: among large smooth curves, all its sectional curvatures are ≥ 0, while for curves with high curvature or pertubations of high frequency, the curvatures are ≤ 0

M. F. Beg, M. I. Miller, A. Trouvé, L. Younes: Computing large deformation metric mappings via geodesic flows of diffeomorphisms, 2003

- images I_0, I_1 are given and connected via the diffeomorphic change of coordinates $I_0 \circ \varphi^{-1} = I_1$
- here $\varphi = \phi_1$ is the end point at $t = 1$ of the curve $(\phi_t)_{t \in [0,1]}$ satisfying $\dot{\phi}_t = v_t(\phi_t)$with $\phi_0 = id$
- the **variational problem** takes the form

$$\mathrm{argmin}_{v:\dot{\phi}_t = v_t(\phi_t)} \Big(\int_0^1 \|v_t\|_V^2 dt + \|I_0 \circ \phi_1^{-1} - I_1\|_{L^2}^2 \Big)$$

  where $\|v_t\|_V$ is an appropriate higher order Sobolev norm
- related to multipolar fluids [Necas, Silhavy '91]

M. Fuchs, B. Jüttler, O. Scherzer, H. Yang: Shape metrics based on elastic deformations,

- For $\mathcal{S} = \partial\mathcal{O}$ define linear "elastic" deformation energy

$$E[u] := \int_{\mathcal{O}} \frac{\lambda}{2} \mathrm{tr}(\epsilon[u])^2 + \mu \mathrm{tr}(\epsilon^2[u])\,\mathrm{d}x$$

- Elastic deformation energy of an infinitesimal boundary deformation:

$$|u_\partial|^2_{e,\mathcal{S}} := \inf_{\substack{u \in H^1(\mathcal{O},\mathbb{R}^2) \\ \mathsf{Tr}u = u_\partial}} E[u]$$

- Let $\mathcal{S}_A, \mathcal{S}_B \in \mathbf{S}$ and $\mathcal{S} : [0,1] \to \mathbf{S}$ piecewise continuously differentiable, then

$$L(\mathcal{S}) := \int_0^1 |\dot{\mathcal{S}}(t)|_{e,\mathcal{S}(t)} dt \text{ and } E(\mathcal{S}) := \int_0^1 |\dot{\mathcal{S}}(t)|^2_{e,\mathcal{S}(t)} dt$$

- explicit triangular finite element mesh for intermediate shapes

- Variational definition of the shape average
- A relaxed formulation
- Applications
- Numerical Implementation
- Generalization of the model

- Input objects

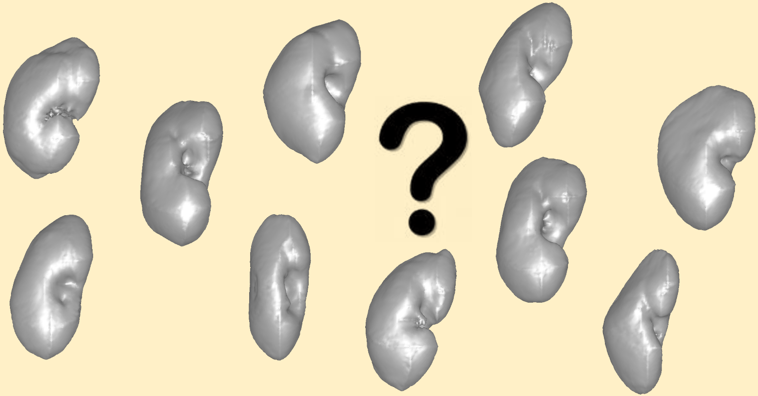

- averaging

$\Longrightarrow$

- dominant modes of variation

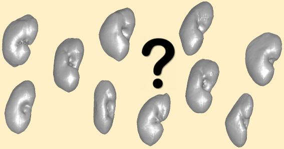

$\Longrightarrow$

- averaging

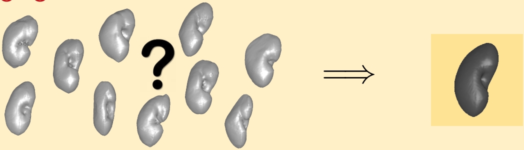

- Variational definition of the shape average
- A relaxed formulation
- Applications
- Numerical Implementation
- Generalization of the model

Recalling the spring model

- given: n points in space x_i, $i = 1, \dots, n$
- classic arithmetic mean: $x = \frac{1}{n}\sum_{i=1}^{n} x_i = \operatorname{argmin}_{\tilde{x}} \sum_{i=1}^{n} (\tilde{x} - x_i)^2$
- $x = \operatorname{argmin}_{\tilde{x}} \sum_{i=1}^{n} E_i$ where $s_i = x - x_i$

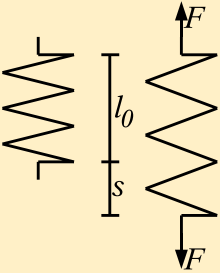

force $F = Ds$
energy $\hat{E} = \frac{D}{2} s^2$

Transfering the spring model to shapes

- consider a one-to-one deformation ϕ from a shape to the (yet unknown) average
- assign an "elastic" energy $\mathcal{W}[\mathcal{O}_i, \phi_i]$ to each deformation
- minimize the accumulated energy

$$\sum_{i=1}^{n} \mathcal{W}[\mathcal{O}_i, \phi_i] \to \min!$$

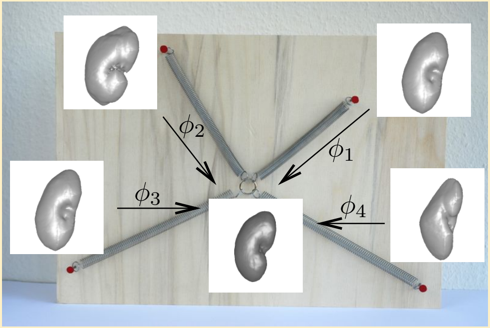

A further example

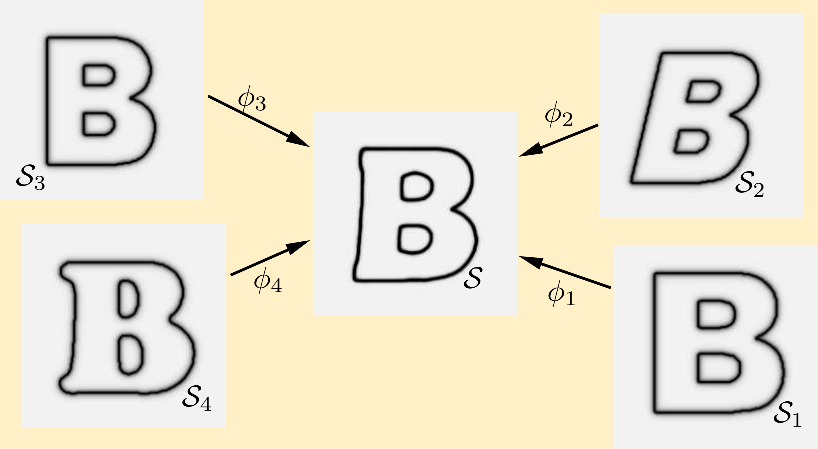

4.1 Definition (Average Shape). *The stored elastic energy of a spring system is given by*

$$\hat{\mathcal{E}}[\mathcal{S},(\phi_i)_{i=1,\ldots,n}] = \begin{cases} \frac{1}{n}\sum_{i=1,\ldots,n} \mathcal{W}[\mathcal{O}_i,\phi_i] & ;\ \phi_i(\mathcal{S}_i) = \mathcal{S} \text{ for } i=1,\ldots,n \\ \infty & ;\ \textit{else}\ . \end{cases}$$

Additionally, an interface regularization $\mathcal{L}$ is added

$$\mathcal{E}[\mathcal{S},(\phi_i)_{i=1,\ldots,n}] = \hat{\mathcal{E}}[\mathcal{S},(\phi_i)_{i=1,\ldots,n}] + \mu\mathcal{L}[\tilde{\mathcal{S}}]\,.$$

Let $\mathcal{A}_{\mathcal{S}}$ be the admissible set of shapes. Then the average shape $\mathcal{S}$ is defined as

$$\mathcal{S} = \operatorname*{arg\,min}_{\tilde{\mathcal{S}}\in\mathcal{A}_{\mathcal{S}},\,\phi_i:\mathcal{O}_i\to\mathbb{R}^d} \mathcal{E}[\tilde{\mathcal{S}},(\phi_i)_{i=1,\ldots,n}]$$

4.2 Theorem (Existence of a shape average). *Let $p > d$ and let the hyperelastic energy density be denoted by W. We assume that*

- *W is polyconvex,*
- *has the form $W(A) = \hat{W}(A, \mathrm{cof}\, A, \det A)$*
- *and satisfies $W(A) \geq C\|A\|_F^p - \tilde{C}$*

for some $C, \tilde{C} > 0$ and for all $A \in \mathbb{R}^{d\times d}$.

Furthermore, assume there exist homeomorphisms $\psi_{kl} \in W^{1,p}(\mathcal{O}_k)$ between $\overline{\mathcal{O}}_k$ and $\overline{\mathcal{O}}_l$ with $\mathcal{W}[\mathcal{O}_k, \psi_{kl}] < \infty$ for all $1 \leq k, l \leq n$.

Then $\mathcal{E}[\mathcal{S}, (\phi_i)_{i=1,\dots,n}]$ admits a minimizing shape $\mathcal{S} \subset \mathbb{R}^d$ and corresponding deformations $\phi_i : \mathcal{O}_i \to \mathbb{R}^d$, $i = 1, \dots, n$.

An existence result (cont.)

Proof.

- $\inf \mathcal{E} < \infty$ due to $\mathcal{E}[\mathcal{S}_l, (\psi_{il})_{i=1,\dots,n}] < \infty$ for $1 \leq l \leq n$.
- Consider a minimizing sequence $(\phi_i^j)_j$ and $\mathcal{S}^j = \phi_i^j(\mathcal{S}_i)$.
- growth conditions on $W \Rightarrow \phi_i^j$ uniformly bounded in $W^{1,p}(\mathcal{O}_i) \Rightarrow$ weakly converging subsequence, strongly in $C^{0,\alpha}(\overline{\mathcal{O}}_i)$ for $\alpha < 1 - \frac{d}{p}$.
- $\phi_l^j \circ \psi_{kl}(\mathcal{S}_k) = \phi_k^j(\mathcal{S}_k) \to \phi_k(\mathcal{S}_k)$
- $\phi_l^j \circ \psi_{kl}(\mathcal{S}_k) \to \phi_l \circ \psi_{kl}(\mathcal{S}_k) = \phi_l(\mathcal{S}_l)$
- Hence, $\phi_k(\mathcal{S}_k) = \phi_l(\mathcal{S}_l) =: \mathcal{S} \quad \forall k, l$ and thus $\mathcal{E}[\mathcal{S}, (\phi_i)_{i=1,\dots,n}] = \frac{1}{n} \sum_{i=1}^n \mathcal{W}[\mathcal{O}_i, \phi_i]$.
- Due to polyconvexity of W, $p > d$ usual weak lower semi continuity applies and thus $\mathcal{E}[\mathcal{S}, (\phi_i)_{i=1,\dots,n}] \leq \liminf_j \mathcal{E}[\mathcal{S}^j, (\phi_i^j)_{i=1,\dots,n}]$ $\Rightarrow$ the minimizer is $(\mathcal{S}, (\phi_i)_{i=1,\dots,n})$.

$\square$

A PDE constrained optimization problem

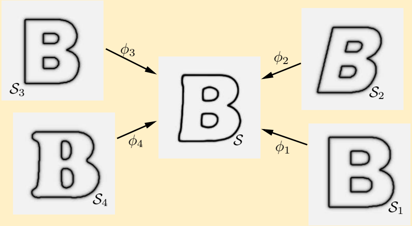

4.3 Remark. *Our approach can be considered as a PDE-constrained shape optimization model:*

We optimize the shape $\mathcal{S}$ with respect to the cost functional

$$\sum_{i=1}^{n} \mathcal{W}[\mathcal{O}_i, \phi_i^*]$$

under the constraint that ϕ_i^* is a minimizer of the functional

$$\phi_i \mapsto \mathcal{W}[\mathcal{O}_i, \phi_i]$$

with $\phi_i(\mathcal{S}_i) = \mathcal{S}$.

4.4 Lemma (Point wise force balance). *The average shape is characterized by the system PDEs* $-\mathrm{div}\, W_{,A}(\mathcal{D}\phi_i) = 0$ *for every deformation* ϕ_i *on* $\mathcal{O}_i \setminus \mathcal{S}_i$ *and the boundary condition*

$$0 = \sum_{i=1,\dots,n} \sigma^{def}[\phi_i](x)\nu[\mathcal{S}](x)$$

Here $\nu[\mathcal{S}](x)$ *is the outer normal on* $\mathcal{S}$ *and*

$$\sigma^{def}[\phi_i] = \left(\sigma[\phi_i](\det \mathcal{D}\phi_i)^{-1}\mathcal{D}\phi_i^T\right) \circ \phi_i^{-1}$$

the Cauchy stress tensor corresponding to the deformation ϕ_i *in the deformed configuration.*

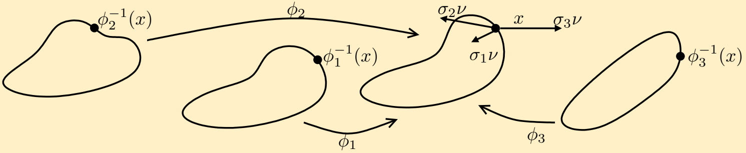

Proof. For the consistent variations $(\mathbb{1}+\epsilon u)\circ\phi_i$ we obtain $\frac{d}{d\epsilon}\sum_{i=1,\dots,n}\mathcal{W}[\mathcal{O}_i,(\mathbb{1}+\epsilon u)\circ\phi_i]\big|_{\epsilon=0}=0$. Hence

$$0=\sum_{i=1,\dots,n}\int_{\mathcal{O}_i}W_{,A}(\mathcal{D}\phi_i):\mathcal{D}(u\circ\phi_i)\,\mathrm{d}x$$

$$=\sum_{i=1,\dots,n}\left(-\int_{\mathcal{O}_i}\mathrm{div}\,W_{,A}(\mathcal{D}\phi_i)(u\circ\phi_i)\,\mathrm{d}x+\int_{\mathcal{S}_i}W_{,A}(\mathcal{D}\phi_i):(u\circ\phi_i)\otimes\nu[\mathcal{S}_i]\,\mathrm{d}a[\mathcal{S}_i]\right)$$

where $\nu[\mathcal{S}_i]$ is the outer normal in $\mathcal{S}_i$ $\Rightarrow$ balance relation between deformation stresses on the averaged shape $\mathcal{S}$:

$$\sum_{i=1,\dots,n}\sigma[\phi_i]\nu[\mathcal{S}_i]\,\mathrm{d}a[\mathcal{S}_i]=0,$$

Finally, by a push forward:

$$\sigma[\phi_i]\nu[\mathcal{S}_i]\,\mathrm{d}a[\mathcal{S}_i]=\sigma^{\mathrm{def}}[\phi_i](x)\nu[\mathcal{S}](x)\,\mathrm{d}a[\mathcal{S}]$$

$\square$

Hyperelastic energy:

$$\mathcal{W}[\phi] = \int_\Omega \hat{W}\left(\mathrm{D}\phi, \mathrm{cof}(\mathrm{D}\phi), \det\left(\mathrm{D}\phi\right)\right)\,\mathrm{d}x$$

- naturally built in frame indifference, measures lack of isometry
- frees us from imposing artificial boundary conditions

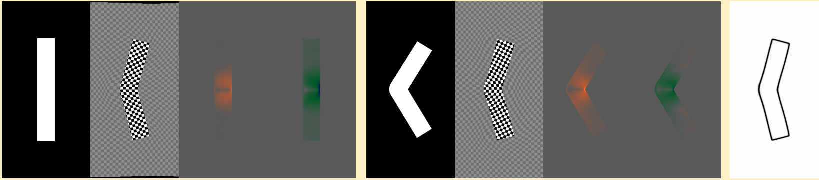

A straight and a folded bar are averaged. The distribution of $|\mathcal{D}\phi_i|_2$ and $\det\left(\mathcal{D}\phi_i\right)$ with ranges of $[0.97\sqrt{2}, 1.03\sqrt{2}]$ and $[0.97, 1.03]$ color-coded as . The original bars describe an angle of $180°$ and $118°$, while the average has an angle of $\approx 150°$. The image resolution is 513×513.

4.5 Definition (inverse model). *Take into account the corresponding inverse maps $\psi_i = \phi_i^{-1}$ and their elastic energy:*

Obviously, $\det \mathcal{D}\psi_i = \frac{1}{\det \mathcal{D}\phi_i}$, $\mathcal{D}\psi_i = \frac{\mathrm{cof}\mathcal{D}\phi_i^T}{\det \mathcal{D}\phi_i}$, *and* $\mathrm{cof}\mathcal{D}\psi_i = \frac{\mathcal{D}\phi_i^T}{\det \mathcal{D}\phi_i}$.

Hence, the elastic energies associated with the inverse deformations ψ_i on the stress-free reference configuration $\mathcal{S}$ are defined as:

$$\mathcal{W}^{inv}[\psi_i] := \int_{\mathcal{O}_i} |\det \mathcal{D}\phi_i|\, \bar{W}\left(\frac{|\mathrm{cof}\mathcal{D}\phi_i|_2^2}{(\det \mathcal{D}\phi_i)^2}, \frac{|\mathcal{D}\phi_i|_2^2}{(\det \mathcal{D}\phi_i)^2}, \frac{1}{\det \mathcal{D}\phi_i}\right) \mathrm{d}x\,,$$

where $\mathcal{W}^{inv}[\psi_i] = \mathcal{W}^{inv}[\mathcal{O}_i, \phi_i]$.

- Variational definition of the shape average
- A relaxed formulation
- Applications
- Numerical Implementation
- Generalization of the model

The hard constraint $\phi_i(\mathcal{S}_i) = \mathcal{S}$ is often inadequate in applications due to local shape fluctuations or noise in the shape acquisition which should not be encountered in the shape average.

4.6 Definition (relaxed variational model). *Consider the mismatch penalty*

$$\mathcal{F}[\mathcal{S}_i, \phi_i, \mathcal{S}] = \mathcal{H}^{d-1}(\mathcal{S}_i \triangle \phi_i^{-1}(\mathcal{S}))\,,$$

where $A \triangle B = A \setminus B \cup B \setminus A$, and the resulting total energy

$$\mathcal{E}^\gamma[\mathcal{S}, (\phi_i)_{i=1,\ldots,n}] = \frac{1}{n} \sum_{i=1}^{n} (\mathcal{W}[\mathcal{O}_i, \phi_i] + \gamma \mathcal{F}[\mathcal{S}_i, \phi_i, \mathcal{S}]) + \mu \mathcal{L}[\mathcal{S}].$$

and define

$$\mathcal{S} = \operatorname*{arg\,min}_{\tilde{\mathcal{S}} \in \mathcal{A}_\mathcal{S},\, \phi_i : \mathcal{O}_i \to \mathbb{R}^d} \mathcal{E}[\tilde{\mathcal{S}}, (\phi_i)_{i=1,\ldots,n}]$$

where $\mathcal{A}_\mathcal{S}$ is an admissible set of shapes.

- shapes may be seen as special cases of images
- consider the edge set/discontinuity set $\mathcal{S}$ of an image u as shape

images u_i

edge sets $\mathcal{S}_i$

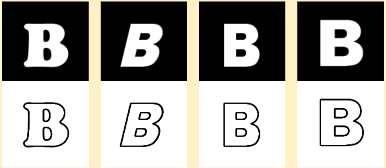

diffused interface: Ambrosio–Tortorelli approximation

$$\mathcal{E}_{\mathrm{AT}}^{\epsilon}[u,v] = \alpha \int_\Omega (u-u_0)^2 \,\mathrm{d}x + \beta \int_\Omega v^2 |\nabla u|^2 \,\mathrm{d}x + \nu \int_\Omega \epsilon |\nabla v|^2 + \frac{1}{4\epsilon}(v-1)^2 \,\mathrm{d}x$$

smooth edge representation:

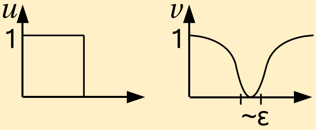

- given n images u_i
- obtain phase fields v_i by Ambrosio-Tortorelli segmentation
- find average phase field $v : \Omega \to \mathbb{R}$ (and corresponding deformations ϕ_i)
- $\phi_i(\mathcal{S}_i) \approx \mathcal{S}$ becomes $v_i \approx v \circ \phi_i$

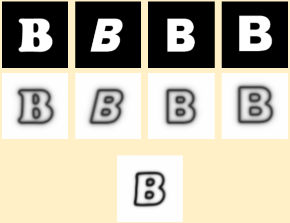

complementarity energy: symmetric edge matching

$$\mathcal{F}^\epsilon[v \circ \phi_i, v_i] = \frac{1}{\epsilon} \int_\Omega (v \circ \phi_i)^2 (1 - v_i)^2 + v_i^2 (1 - v \circ \phi_i)^2 \,\mathrm{d}x$$

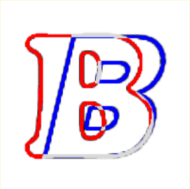

$$\mathcal{L}^\epsilon[v] = \frac{1}{2} \int_\Omega \epsilon |\nabla v|^2 + \frac{1}{4\epsilon}(v-1)^2 \,\mathrm{d}x$$

Energies in the phase field model

hyperelastic energy

$$\mathcal{W}[\mathcal{O},\phi] = \int_{\mathcal{O}} \hat{W}\left(\mathrm{D}\phi, \mathrm{cof}\,\mathrm{D}\phi, \det \mathrm{D}\phi\right)\,\mathrm{d}x$$

$$\hat{W}(A,C,D) = a_1|A|^p + a_2|C|^q + \Gamma(D)$$

complementarity energy and regularization

$$\mathcal{F}^\epsilon[v\circ\phi_i, v_i] = \frac{1}{\epsilon}\int_\Omega (v\circ\phi_i)^2(1-v_i)^2 + v_i^2(1-v\circ\phi_i)^2\,\mathrm{d}x$$

$$\mathcal{L}^\epsilon[v] = \int_\Omega \epsilon|\nabla v|^2 + \frac{1}{4\epsilon}(v-1)^2\,\mathrm{d}x$$

shape averaging functional

$$\mathcal{E}[v,\phi_1,\ldots,\phi_n] = \sum_{i=1}^n \left(\mathcal{W}[\mathcal{O}_i,\phi_i] + \gamma F^\epsilon[v\circ\phi_i, v_i] + \mu L^\epsilon[v]\right)$$

$\gamma \gg 1,\ \mu \ll 1$

soft material outside ($\delta = 10^{-4}$):

$$\mathcal{W}^{\epsilon,\delta}[\mathcal{O}_i, \phi_i] = \int_\Omega \Big((1-\delta)\chi^\epsilon_{\mathcal{O}_i} + \delta \Big) W(\mathrm{D}\phi_i)\, \mathrm{d}x \,,$$

where $\chi^\epsilon_{\mathcal{O}_i}$ is a smooth approximation of $\chi_{\mathcal{O}_i}$.

Impact of the choice of the effective elastic domain:

$\delta = 10^{-4}$:

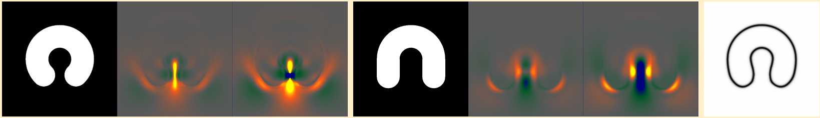

$\delta = 1$:

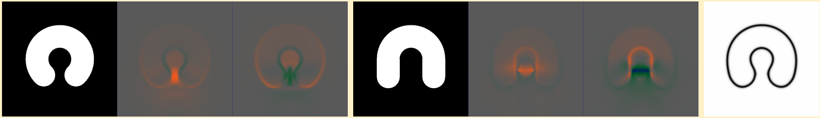

4.7 Theorem (existence of a phase field shape average). *Suppose $d = 3$, $\epsilon, \delta, \gamma, \mu > 0$, and consider a set of admissible deformations*

$$\begin{aligned} \mathcal{A} \quad := \quad & \{\phi : \Omega \to \Omega \,\big|\, \phi \in W^{1,p}(\Omega), \mathrm{cof} D\phi \in L^q(\Omega), \\ & \det D\phi \in L^r(\Omega), \det D\phi > 0 \text{ a.e. in } \Omega, \phi = 1\!\!1 \text{ on } \partial\Omega\} \end{aligned}$$

on a uniform image domain $\Omega = [0,1]^3$, where p, $q > 3$ and $r > 1$. We assume $\bar{W}$ is convex and the growth condition such that $\hat{W}(A, C, D) \geq \kappa(|A|^p + |C|^q + D^r + D^{-s})$ holds for $\kappa > 0$ and $s > \frac{2q}{q-3}$. If the input phase fields $(v_i)_{i=1,\ldots,n}$ lie in $W^{1,2}(\Omega)$ with $0 \leq v_i \leq 1$, then the energy

$$\mathcal{E}^\epsilon[v, (\phi_i)_{i=1,\ldots,n}] = \frac{1}{n} \sum_{i=1}^{n} \left(\mathcal{W}^{\epsilon,\delta}[\mathcal{O}_i, \phi_i] + \gamma \mathcal{F}^\epsilon[v_i, \phi_i, v] \right) + \mu \mathcal{L}^\epsilon[v]$$

attains its minimum over $v \in W^{1,2}(\Omega)$ and $(\phi_i)_{i=1,\ldots,n}$ in $\mathcal{A}^n$. Furthermore, $v \in C^{1,\alpha}(\bar{\Omega})$, $\phi_i \in C^{0,\beta}(\bar{\Omega})$, $v \circ \phi_i \in C^{0,\beta}$ for all $0 < \alpha < 1 - \frac{3}{s+1}$, $0 < \beta < 1 - \frac{3}{p}$ and the minimizing deformations are homeomorphisms.

Existence of a minimizer for the relaxed model

Proof. $\mathcal{E}[v,\phi_1,\dots,\phi_n] = \sum_{i=1}^{n}\Big(\int_\Omega \hat{W}\left(\mathrm{D}\phi_i, \mathrm{cof}\mathrm{D}\phi_i, \det\mathrm{D}\phi_i\right)\,\mathrm{d}x$

$$+\frac{\gamma}{\epsilon}\int_\Omega (v\circ\phi_i)^2(1-v_i)^2+v_i^2(1-v\circ\phi_i)^2\,\mathrm{d}x + \mu\int_\Omega \epsilon|\nabla v|^2+\frac{1}{4\epsilon}(v-1)^2\,\mathrm{d}x\Big)$$

$W[\mathcal{D}\phi] \geq \kappa(|\mathcal{D}\phi|^p+|\mathrm{cof}\mathcal{D}\phi|^q+\det\mathcal{D}\phi^r+\det\mathcal{D}\phi^{-s})$, $p,q>3$, $s>\frac{2q}{q-3}$, $r>1$

- energy not infinite and bounded below
- minimizing sequence $(v^k,\phi_1^k,\dots,\phi_n^k)$
- $\det\mathrm{D}\phi_i^k > 0$ a.e., ϕ_i^k bounded in $W^{1,p}(\Omega)$, ϕ_i^k homeomorphism (cf. [Ball'83])
- byproduct: transformation rule $\int_\Omega f\circ\phi_i^k \det\mathcal{D}\phi_i^k\,\mathrm{d}x = \int_{\phi_i^k(\Omega)} f\,\mathrm{d}x$
- replace v^k by $\mathrm{argmin}_v\,\mathcal{E}[v,\phi_1^k,\dots,\phi_n^k]$
- Euler-Lagrange:

$$-\epsilon\mu\Delta v^k = -\frac{\mu}{4\epsilon}(v^k-1)-\frac{\gamma}{\epsilon}\sum_{i=1}^{n}\Big((v^k\circ\phi_i^k)(1-v_i)^2+(v^k\circ\phi_i^k-1)v_i^2\Big)\,|\det\mathcal{D}(\phi_i^k)^{-1}|$$

- new v^k bounded in $L^\infty(\Omega)\cap W^{2,s+1}$ with $v^k(x)\in[0,1]$
- sequential weak lower semi-continuity for $(v^k,\phi_i^k)\rightharpoonup(v,\phi_i)$ $\square$

- Variational definition of the shape average
- A relaxed formulation
- Applications
- Numerical Implementation
- Generalization of the model

Averaging B's

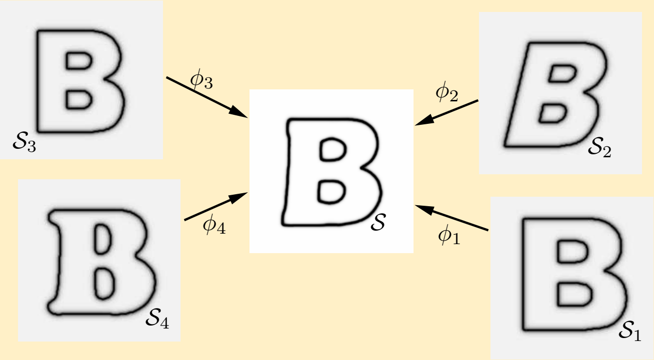

Resolution 257×257 and parameters $\gamma = 10^7$, $\mu = 1$, $(a_1, a_2, a_3) = (10^6, 0, 10^6)$.

Averaging 2D silhouettes

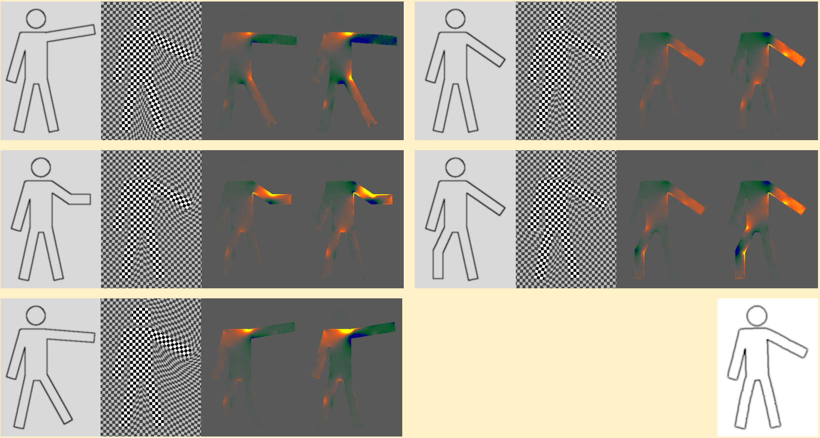

resolution 513×513, and parameters $\gamma = 10^7$, $\mu = 10^{-2}$,
$(a_1, a_2, a_3) = (10^{10}, 0, 10^{10})$

Shape averaging examples (cont.)

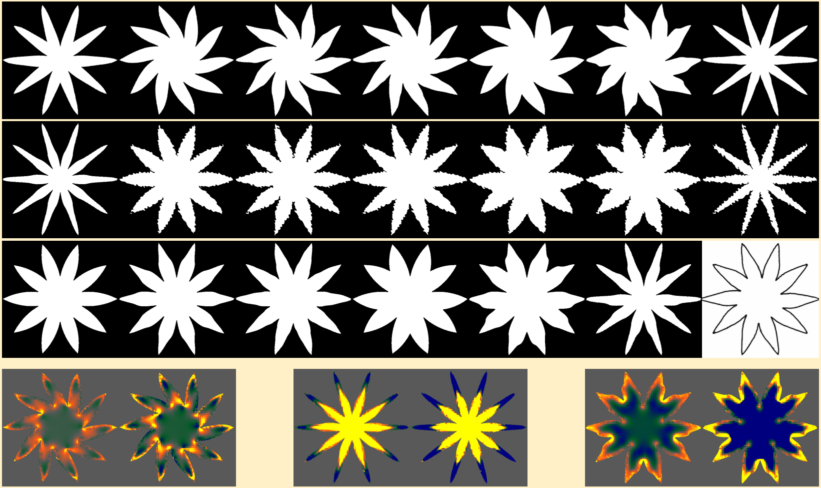

20 shapes “device7” from the MPEG7 shape database and their average phase field.

Further 2D examples (cont.)

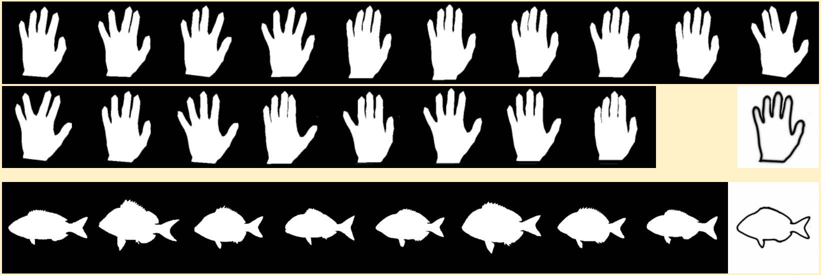

18 hand and 8 fish silhouettes ([Cootes, Taylor, Cooper,Graham '95] shape database at the Centre for Vision, Speech, and Signal Processing, University of Surrey)

Further 2D examples (cont.)

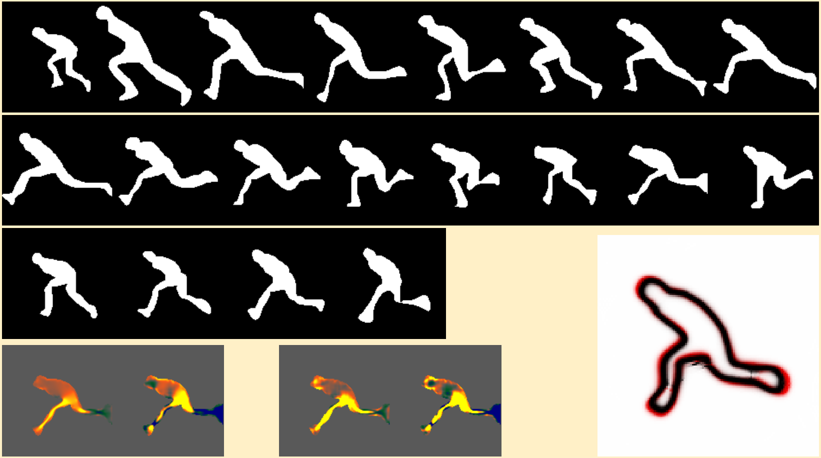

20 shapes “stef” from the MPEG7 shape database and their average phase field (bottom right) for elastic parameters $(a_1, a_2, a_3) = (10^7, 0, 10^6)$ (black) and $(a_1, a_2, a_3) = (10^5, 0, 10^6)$ (red)

(resolution 129×129, $\gamma = 10^7$, $\mu = 10^{-2}$)

Average of 3D kidneys

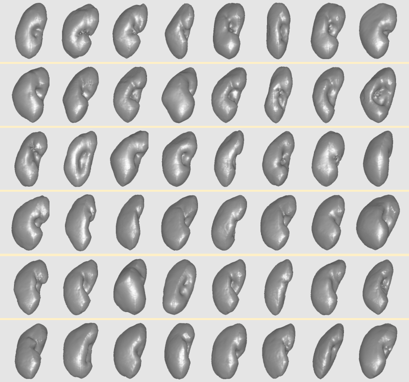

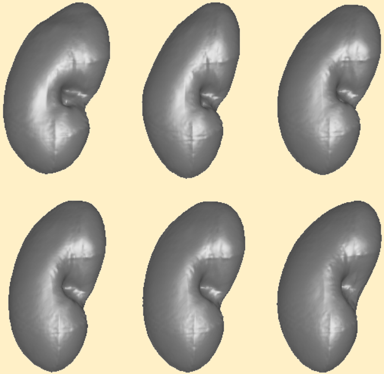

The averaged shape of the first two, four, five, six, eight and of all 48 kidneys are depicted.

Average of 3D kidneys (cont.)

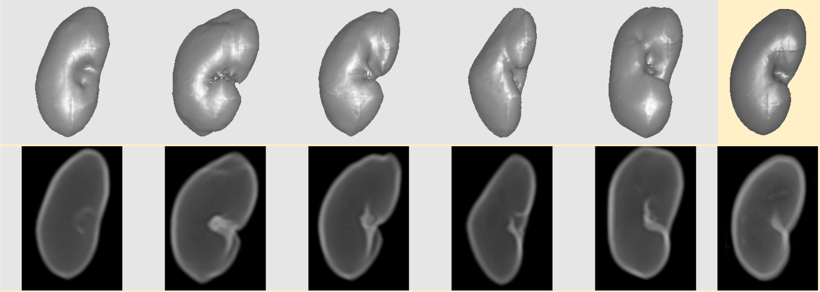

Five kidneys and their average (right).

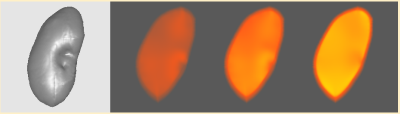

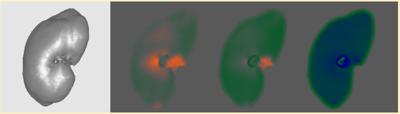

Average of 3D scanned feet

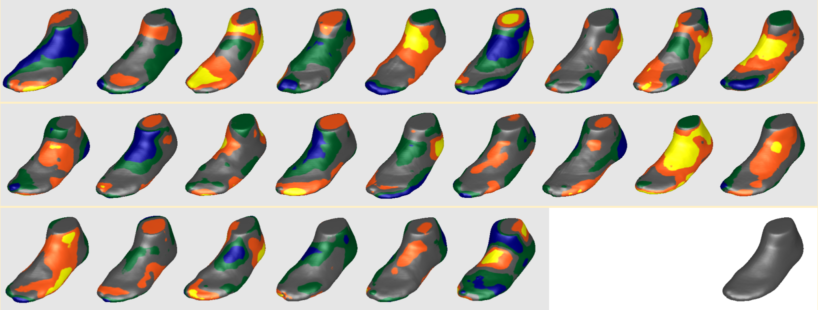

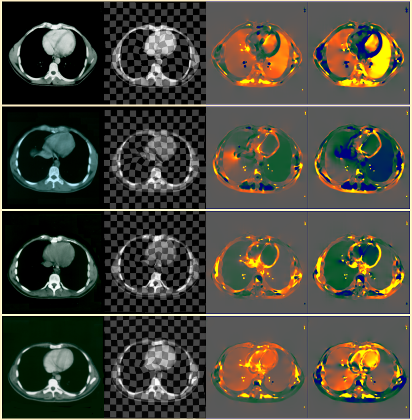

Averaging CT scan slices of the thorax from four different patients, from left to right: original image, ϕ_i, $|\mathcal{D}\phi_i|_2$, and $\det(\mathrm{D}\phi_i)$ (resolution 257×257 and parameters $\gamma = 10^7$, $\mu = 0.1$, $(a_1, a_2, a_3) = (10^6, 0, 10^6)$.)

- Variational definition of the shape average
- A relaxed formulation
- Applications
- Numerical Implementation
- Generalization of the model

For the total energy

$$\mathcal{E}^\epsilon[v,(\phi_i)_{i=1,\dots,n}] = \frac{1}{n}\sum_{i=1}^{n}\left(\mathcal{W}^{\epsilon,\delta}[\mathcal{O}_i,\phi_i] + \gamma\mathcal{F}^\epsilon[v_i,\phi_i,v]\right) + \mu\mathcal{L}^\epsilon[v]$$

we compute $\delta_v\mathcal{E}^\epsilon = \frac{\gamma}{n}\sum_{i=1}^n \delta_v\mathcal{F}^\epsilon + \mu\delta_v\mathcal{L}^\epsilon$ and $\delta_{\phi_i}\mathcal{E}^\epsilon = \frac{1}{n}\sum_{i=1}^n(\delta_{\phi_i}\mathcal{W}^\epsilon + \gamma\delta_{\phi_i}\mathcal{F}^\epsilon)$ with

$$\langle\delta_v\mathcal{F}^\epsilon,\vartheta\rangle = \frac{2}{\epsilon}\int_{\phi_i(\Omega)}\left(v(1-v_i\circ\phi_i^{-1})^2-(v_i\circ\phi_i^{-1})^2(1-v)\right)\cdot\vartheta\,|\det(\mathrm{D}\phi_i^{-1})|\,\mathrm{d}x$$

$$\langle\delta_{\phi_i}\mathcal{F}^\epsilon,\psi\rangle = \frac{2}{\epsilon}\int_\Omega\left((1-v_i)^2(v\circ\phi_i) - v_i^2(1-v\circ\phi_i)\right)(\nabla v\circ\phi_i)\cdot\psi\,\mathrm{d}x$$

$$\langle\delta_v\mathcal{L}^\epsilon,\vartheta\rangle = 2\int_\Omega \epsilon\nabla v\cdot\nabla\vartheta + \frac{1}{4\epsilon}(v-1)\vartheta\,\mathrm{d}x$$

$$\langle\delta_{\phi_i}\mathcal{W}^{\epsilon,\delta},\psi\rangle = \int_\Omega\Big((1-\delta)\chi^\epsilon_{\mathcal{O}_i}+\delta\Big)W_{,A}(\mathrm{D}\phi_i):\mathrm{D}\psi\,\mathrm{d}x$$

Variation of the energy (cont.)

fully enrolling the derivatives:

if $\hat{W}(A,C,D) = \bar{W}(|A|^2, |C|^2, D)$ and
$\bar{W}(I_1, I_2, I_3) = a_1(I_1 - 3)^{\frac{p}{2}} + a_2(I_2 - 3)^{\frac{q}{2}} + a_3\left(I_3^{-s} + \frac{s}{r}I_3^r - \frac{r+s}{r}\right)$ then

$$\begin{aligned} W_{,A}(A) : B &= 2\,\partial_{I_1}\bar{W}(|A|_2^2, |\mathrm{cof}\,A|_2^2, \det A)\; A : B + \\ & \quad 2\,\partial_{I_2}\bar{W}(|A|_2^2, |\mathrm{cof}\,A|_2^2, \det A)\; \mathrm{cof}\,A : \partial_A \mathrm{cof}(A)(B) + \\ & \quad \partial_{I_3}\bar{W}(|A|_2^2, |\mathrm{cof}\,A|_2^2, \det A)\; \partial_A \det(A)(B)\,, \end{aligned}$$

$$\begin{aligned} \partial_A \det(A)(B) &= \det(A)\mathrm{tr}\,(A^{-1}B)\,, \\ \partial_A \mathrm{cof}(A)(B) &= \det(A)\mathrm{tr}\,(A^{-1}B)A^{-T} - \det(A)A^{-T}B^TA^{-T}. \end{aligned}$$

Space discretization via finite elements

- Consider images u_i, phase fields v, v_i, and deformations ϕ_i as being represented by continuous, piecewise multilinear (trilinear in 3D and bilinear in 2D) finite element functions on $\Omega = [0,1]^d$
- denote discrete quantities by U_i, V, V_i, Φ_i, e.g. $\mathbf{V} = (\mathbf{V}_j)_{j \in I_h}$ with $V = \sum_{j \in I_h} \mathbf{V}_j \varphi_j$ where $\{\varphi_j\}_{j \in I_h}$ is the nodal basis and I_h the grid node index set
- For ease of implementation we suppose dyadic resolutions of the images with $2^L + 1$ pixels or voxels in each direction corresponding to a grid size $h = 2^{-L}$.
- $\Phi = \sum_{j \in I_h} \sum_{j=1,\ldots,d} \mathbf{\Phi}_{jk} \varphi_j e_k$, where $e_1, \ldots, e_d$ is the canonical basis in $\mathbb{R}^d$

Space discretization via finite elements (cont.)

$$0 = \delta_v \mathcal{E}^\epsilon = \tfrac{\gamma}{n} \sum_{i=1}^n \delta_v \mathcal{F}^\epsilon + \mu \delta_v \mathcal{L}^\epsilon \longrightarrow$$

$$0 = \left(\frac{\gamma}{n\epsilon} \sum_{i=1}^n M \left[\left((1 - V_i \circ \Phi_i^{-1})^2 + (V_i \circ \Phi_i^{-1})^2 \right) \det \mathcal{D}\Phi_i^{-1} \right] + \mu\epsilon L + \frac{\mu}{4\epsilon} M[1] \right) \mathbf{V}$$
$$- \left(\frac{\gamma}{n\epsilon} \sum_{i=1}^n M \left[(V_i \circ \Phi_i^{-1})^2 \det \mathcal{D}\Phi_i^{-1} \right] + \frac{\mu}{4\epsilon} M[1] \right) \underline{\mathbf{1}} =: A_{V_i,\Phi_i} \mathbf{V} - b_{V_i,\Phi_i},$$

where the generalized mass matrix $M[\omega]$ and the matrix L are defined as

$$M[\omega] = \left(\int_\Omega \omega \varphi_i \varphi_j \, \mathrm{d}x \right)_{ij}, \quad L = \left(\int_\Omega \omega \nabla\varphi_i \cdot \nabla\varphi_j \, \mathrm{d}x \right)_{ij},$$

$\leftrightarrow$ linear in $\mathbf{V}$, nonlinear in $\mathbf{\Phi_i}$

Space discretization via finite elements (cont.)

$$0 = \delta_{\phi_i}\mathcal{E}^\epsilon = \tfrac{1}{n}\sum_{i=1}^{n}(\delta_{\phi_i}\mathcal{W}^\epsilon + \gamma\delta_{\phi_i}\mathcal{F}^\epsilon) \longrightarrow$$

$$\begin{aligned} 0 \;=\; & \frac{2\gamma}{n\epsilon}\int_\Omega \big((1-V_i)^2(V\circ\Phi_i) - V_i^2(1-V\circ\Phi_i)\big)\,\Psi\cdot(\nabla V\circ\Phi_i)\,\mathrm{d}x \\ & + \frac{1}{n}\int_\Omega \Big((1-\delta)\chi^\epsilon_{\mathcal{O}_i} + \delta\Big) W_{,A}(\mathcal{D}\Phi_i) : \mathcal{D}\Psi\,\mathrm{d}x \end{aligned}$$

nonlinear in Φ_i

- perform a fixed point iteration, alternatingly updating $\mathbf{V}$ and Φ_i
- Equation resulting from $0 = \delta_v\mathcal{E}^\epsilon$ is linear in the vector $\mathbf{V}$ for fixed deformations Φ_i and therefore solved by conjugate gradient iteration.
- Resort to a regularized gradient descent to update $\mathbf{\Phi}_i$ according to

$$\Phi_i = \Phi_i^{\text{old}} - \tau\,\mathrm{grad}_{\Phi_i}\mathcal{E}_h^{\gamma,\epsilon},$$

with respect to the weighted H^1 inner product

$$(\Psi_1,\Psi_2)_\sigma := (\Psi_1,\Psi_2)_{L^2} + \frac{\sigma^2}{2}(\mathcal{D}\Psi_1,\mathcal{D}\Psi_2)_{L^2}\,.$$

Computing pull back and push forward under a deformation

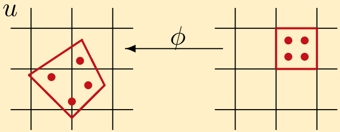

pull back functionals $\int_\Omega f(U \circ \Phi)\,\mathrm{d}x$

- exact evaluation at quadrature points

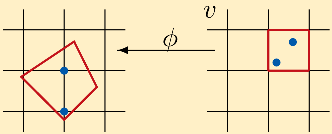

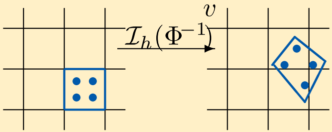

push forward functionals $\int_\Omega f(V \circ \Phi^{-1})\,\mathrm{d}x$

- $\int_\Omega f(\mathcal{I}_h(V \circ \Phi^{-1}))\,\mathrm{d}x$ not sufficient
- compute $\mathcal{I}_h(\Phi^{-1})$:
  - for each grid cell C
    identify nodes $N_i \in \Phi(C)$
    ($O(1)$ on a structured grid)
  - Newton iteration for $\Phi^{-1}(N_i)$
- compute $\int_\Omega f(V \circ \mathcal{I}_h(\Phi^{-1}))\,\mathrm{d}x$ as above

Computation cost for an example

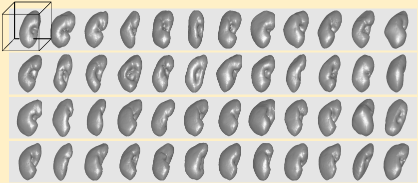

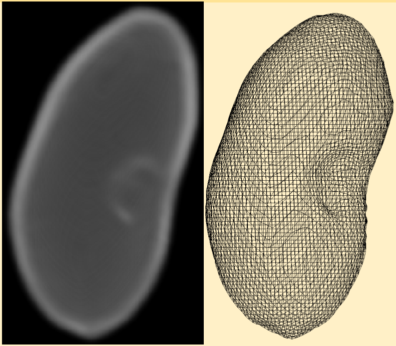

- 257^3 grid nodes
- 48 data sets
- each with 1 phase field
  3D deformation

$\sim 3 \cdot 10^9$ dofs (12 GB in case of 4 byte per dof)

remarks on the implementation:

- problems on multiple scales

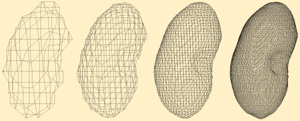

- alternating gradient descent $\longleftrightarrow$ easy to run in parallel

EnergyRelaxation $\left((U_i^0)_{i=1,\dots,n}\right)$
initialize $\mathbf{\Phi}_i = \mathbb{1}$ on grid level l_0 for all $i = 1,\dots,n$;
for grid level $l = l_0$ to L {
do {
segment the images $(U_i^0)_{i=1,\dots,n}$ to obtain phase fields $(V_i)_{i=1,\dots,n}$;
$\mathbf{V}^{\text{old}} = \mathbf{V}$;
solve the linear system
$A_{V_i,\Phi_i}\mathbf{V} = b_{V_i,\Phi_i}$ for the phase field vector $\mathbf{V}$;
for image $i = 1$ to n
for count $k = 1$ to K {
$\mathbf{\Phi}_i^{\text{old}} = \mathbf{\Phi}_i$;
perform a gradient descent step
$\mathbf{\Phi}_i = \mathbf{\Phi}_i^{\text{old}} - \tau\, \mathrm{grad}_{\mathbf{\Phi}_i^{\text{old}}} \mathcal{E}_h^{\gamma,\epsilon}[\mathbf{V}, (\mathbf{\Phi}_j)_{j=1,\dots,n}]$
with Armijo step size control for τ; }
} **while**$(\sum_{i=1}^n |\mathbf{\Phi}_i^{\text{old}} - \mathbf{\Phi}_i| + |\mathbf{V}^{\text{old}} - \mathbf{V}| \geq$ Threshold);
if $(l < L)$ prolongate $\mathbf{V}$, $\mathbf{\Phi}_i$ for all $i = 1,\dots,n$ onto the next grid level;
}

Energy decay in the algorithm

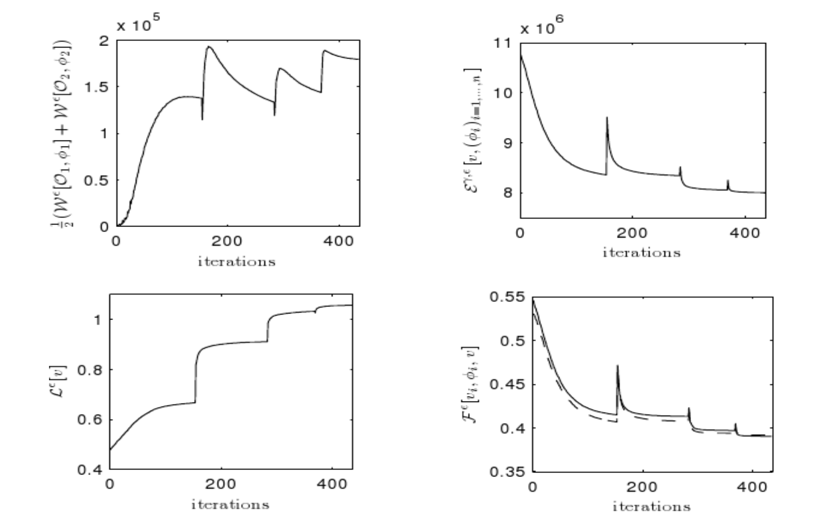

- Variational definition of the shape average
- A relaxed formulation
- Applications
- Numerical Implementation
- Generalization of the model

modified averaging functional:

$$\mathcal{E}^{\gamma,\epsilon}[v,(\phi_i)_{i=1,\ldots,n}] = \sum_{i=1}^{n} \left(\lambda_i \mathcal{W}^{\epsilon}[\mathcal{O}_i, \phi_i] + \frac{\gamma}{n} \mathcal{F}^{\epsilon}[v_i, \phi_i, v] \right) + \mu \mathcal{L}^{\epsilon}[v]\,,$$

with $\lambda_i > 0$ and $\sum_{i=1}^{n} \lambda_i = 1$

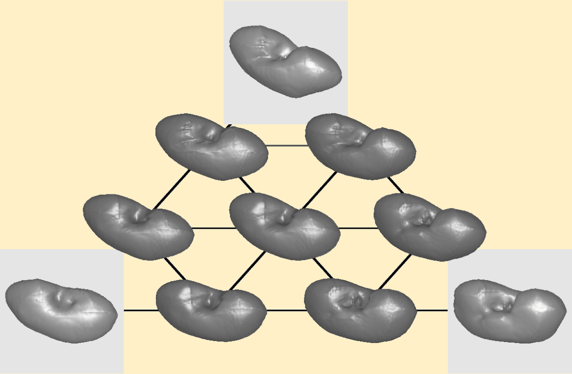

So far the shapes $\mathcal{S}_i$ are assumed to be robustly extracted from a set of images u_i with $i = 1, \ldots, n$ and are a priori given.

However, image edges may be characterized by significant noise or low contrast and hence will be difficult to extract.

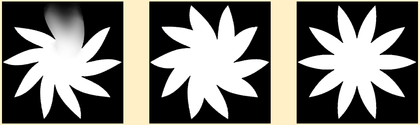

Alternative: Joint approach of shape segmentation and registration with an averaged shape:

- the quality of shape averaging highly depends on the robustness of the edge detection in the input images
- a reliable average shape can be used to improve edge detection in case of poor image quality

For shape segmentation we pick up the Mumford and Shah approach for input images u^0 on an image domain Ω:

$$\mathcal{E}_{\mathsf{MS}}[u,\mathcal{S},u^0] = \alpha \int_\Omega (u-u^0)^2 \,\mathrm{d}x + \beta \int_{\Omega\setminus\mathcal{S}} |\nabla u|^2 \,\mathrm{d}x + \nu \mathcal{H}^{d-1}(\mathcal{S}),$$

and end up with the joint functional

$$\begin{aligned}\mathcal{E}_{\mathsf{joint}}[\mathcal{S},(u_i,\mathcal{S}_i,\phi_i)_{i=1,\dots,n}] \;=\; & \frac{1}{n}\sum_{i=1}^{n}\left(\mathcal{E}_{\mathsf{MS}}[u_i,\mathcal{S}_i,u_i^0]+\mathcal{W}[\Omega,\phi_i]+\gamma\mathcal{F}[\mathcal{S}_i,\phi_i,\mathcal{S}]\right)\\ & +\mu\mathcal{L}[\mathcal{S}],\end{aligned}$$

Task: Relax simultaneously in the unknowns u_i, $\mathcal{S}_i$, ϕ_i for $i = 1,\dots,n$ and $\mathcal{S}$ for a fixed given set of input images $(u_i^0)_{i=1,\dots,n}$

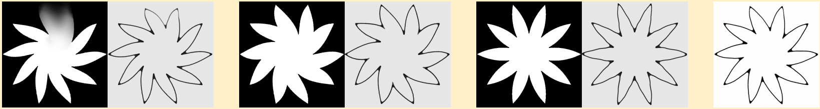

resolution 513×513, $\gamma = 10^7$, $\mu = 10^{-2}$, $(a_1,a_2,a_3) = (10^8, 0, 10^8)$, $\alpha = 10^{10}$, $\beta = 10^5$, $\nu = 10^6$.

$$\mathcal{E}^{\epsilon}_{\text{joint}}[v,(u_i,v_i,\phi_i)_i]=\frac{1}{n}\sum_{i=1}^{n}\Big(\mathcal{E}^{\epsilon}_{\text{AT}}[u_i,v_i,u_i^0]+\mathcal{W}^{\epsilon}[\Omega,\phi_i]+\gamma\mathcal{F}^{\epsilon}[v_i,\phi_i,v]\Big)+\mu\mathcal{L}^{\epsilon}[v]$$

4.8 Theorem. *Under the above assumption and for $u_i^0 \in L^2(\Omega)$ for $i = 1, \dots, n$ the energy*

$$\mathcal{E}^{\epsilon}_{\textit{joint}}[v, (u_i, v_i, \phi_i)_{i=1,\dots,n}]$$

attains its minimum over n-tupels of images $u_i \in W^{1,2}(\Omega)$, phase fields $v_i \in W^{1,2}(\Omega)$, and deformations $\phi_i \in \mathcal{A}$ with $i = 1, \dots n$, and over phase fields $v \in W^{1,2}(\Omega)$. Finally, for the minimizer $v_i \in C^{1,\alpha'}(\bar{\Omega})$, $v \in C^{1,\alpha''}(\bar{\Omega})$, $\phi_i \in C^{0,\beta'}(\bar{\Omega})$, $v \circ \phi_i \in C^{0,\beta'}$ for all $0 < \alpha' < 1$, $0 < \alpha'' < 1 - \frac{3}{s+1}$, $0 < \beta' < 1 - \frac{3}{p}$ and the minimizing deformations are homeomorphisms.

- General set up
- Linear shape variations
- The actual covariance analysis
- Applications

- General set up
- Linear shape variations
- The actual covariance analysis
- Applications

- averaging

$\Longrightarrow$

- dominant modes of variation

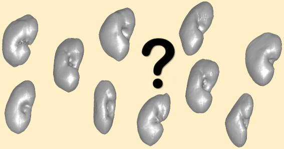

$\Longrightarrow$

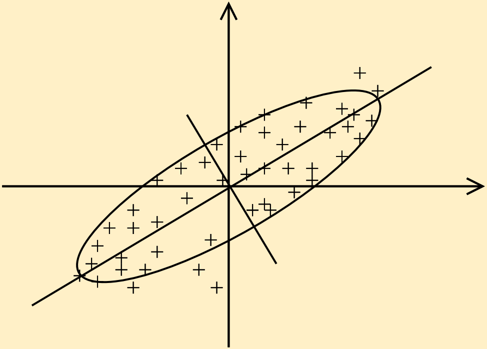

[Cootes, Taylor, Cooper, Graham '95]

data points $X = (x_1|\ldots|x_n)$

correlation matrix $C = \frac{1}{n}(x_i \cdot x_j)_{ij} = \frac{1}{n}X^T X$

matrix decomposition $C = O\Lambda O^{\mathrm{T}}$

modes of variation $Y = XO\sqrt{\Lambda^{-1}}$

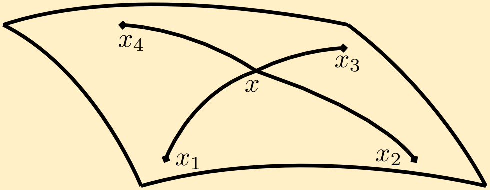

inner product
$\langle\cdot,\cdot\rangle_y$ in $\mathcal{T}_y\mathcal{M}$

geodesic distance
$d(\cdot,\cdot)$

average
$x = \underset{\tilde{x}}{\operatorname{argmin}} \sum_{i=1}^n d(\tilde{x}, x_i)^2$

linear representative
$v_i \in \mathcal{T}_x\mathcal{M}$ with $x_i = \exp_x(v_i)$

[Fletcher, Lu, Joshi '03]
[Charpiat, Faugeras, Keriven '03]
[Fuchs, Jüttler, Scherzer, Yang '09]
[Miller, Trouvé, Younes '02]

data points	$X = (v_1\| \dots \|v_n)$
correlation matrix	$C = (\frac{1}{n} g_x(v_i, v_j))_{ij}$
matrix decomposition	$C = O\Lambda O^{\mathrm{T}}$
modes of variation	$Y = XO\sqrt{\Lambda^{-1}}$

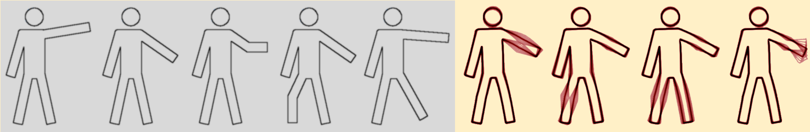

Outline:

- represent shapes via a mode of variation in a linear space:
  variation of the average shape via a displacement
- scalar product on these modes:
  best physically motivated on the prestressed average object
- singular value decomposition of the modes:
  physically sound dominant displacement modes

⟶ can be used for further statistical analysis

⟶ allows to define a new distance measure from a set of training data

- General set up
- Linear shape variations
- The actual covariance analysis
- Applications

Boundary stresses as a representation of shape variations

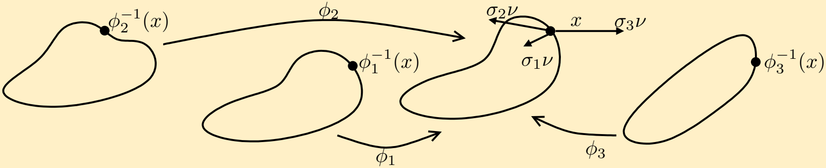

By the Cauchy stress principle, each deformation $\phi_i : \mathcal{O}_i \to \mathcal{O}$ is characterized by pointwise boundary stresses $\sigma_i\nu$ on $\mathcal{S}$:

- The resulting stress $\sigma_i\nu$ is a force density acting $\mathcal{S}$.
- $\mathcal{S}$ is in equilibrium if the opposite force is applied as external load.
- The average shape can be described in terms of the input shape $\mathcal{S}_i$ and the boundary stress $\sigma_i\nu$, and we write $\mathcal{S} = \mathcal{S}_i[\sigma_i\nu]$.
- There is an associated one-parameter family of shapes $\mathcal{S}(t) = \mathcal{S}_i[t\sigma_i\nu]$ connecting $\mathcal{S}_i = \mathcal{S}(0)$ with $\mathcal{S} = \mathcal{S}(1)$.

Characterization of the shape average by the point wise balance relation:

$$0 = \sum_{i=1,\dots,n} \sigma_i(x)\nu(x)$$

How to compute a representing displacement for the family $\mathcal{S}_i[t\sigma_i\nu]$?

Apply the Cauchy stress $\delta\sigma_k\nu$ to the average shape $\mathcal{S}$ ($\delta << 1$) and define the perturbed energy

$$\mathcal{E}_k[\delta, u] = \frac{1}{n}\sum_{i=1}^{n} \mathcal{W}[\mathcal{O}_i, (\mathbb{1}+\delta u)\circ\phi_i] - \delta^2 \int_{\mathcal{S}} \sigma_k\nu\cdot u \,\mathrm{d}a \ .$$

Define a displacement u_k as the minimizer of $\mathcal{E}_k[\delta, u]$ for fixed deformations $(\phi_i)_{i=1,\ldots,n}$ under the constraints $\int_{\mathcal{O}} u_k \,\mathrm{d}x = 0$ and $\int_{\mathcal{O}} x \times u_k \,\mathrm{d}x = 0$.

5.1 Lemma (Euler–Lagrange condition for u_k). *The scaled displacement $\delta\, u_k$ solves $-\mathrm{div}\, \sigma[\delta\, u_k] = 0$ on $\mathcal{O}$ and $\sigma[\delta\, u_k]\nu = \delta\sigma_k\nu$ on $\mathcal{S}$ with*

$$\sigma[\delta\, u_k] := \frac{1}{n}\sum_{i=1}^{n} W_{,A}((\mathbb{1}+\delta\mathcal{D}u_k)\mathcal{D}\phi_i\circ\phi_i^{-1})\mathrm{cof}\mathcal{D}(\phi_i^{-1})$$

the first Piola–Kirchhoff stress tensor on the compound object $\mathcal{O}$.

Displacements representing shape variations (cont.)

Proof. Abbreviating $\psi_k := \mathbb{1} + \delta u_k$, the optimality condition reads

$$
\begin{aligned}
0 &= \langle \partial_{\psi_k} \mathcal{E}_k, \psi \rangle \\
&= \frac{1}{n} \sum_{i=1}^{n} \int_{\mathcal{O}_i} W_{,A}(\mathcal{D}(\psi_k \circ \phi_i)) : \mathcal{D}\psi \circ \phi_i \mathcal{D}\phi_i \,\mathrm{d}x - \delta \int_{\mathcal{S}} (\sigma_k \nu) \cdot \psi \,\mathrm{d}a \\
&= \frac{1}{n} \sum_{i=1}^{n} \int_{\mathcal{O}} W_{,A}(\mathcal{D}\psi_k \mathcal{D}\phi_i \circ \phi_i^{-1}) \mathrm{cof} \mathcal{D}(\phi_i^{-1}) : \mathcal{D}\psi \,\mathrm{d}x - \delta \int_{\mathcal{S}} (\sigma_k \nu) \cdot \psi \,\mathrm{d}a \\
&= \int_{\mathcal{O}} \sigma[\delta\, u_k] : \mathcal{D}\psi \,\mathrm{d}x - \delta \int_{\mathcal{S}} (\sigma_k \nu) \cdot \psi \,\mathrm{d}a \\
&= \int_{\mathcal{S}} ((\sigma[\delta\, u_k] - \delta \sigma_k)\nu) \cdot \psi \,\mathrm{d}a - \int_{\mathcal{O}} \mathrm{div}\, \sigma[\delta\, u_k] \cdot \psi \,\mathrm{d}x
\end{aligned}
$$

for all test functions ψ, where

$$
\sigma[\delta\, u_k] := \frac{1}{n} \sum_{i=1}^{n} W_{,A}((\mathbb{1} + \delta \mathcal{D} u_k) \mathcal{D}\phi_i \circ \phi_i^{-1}) \mathrm{cof} \mathcal{D}(\phi_i^{-1})
$$

Hence, as Euler–Lagrange condition for u_k we obtain $-\mathrm{div}\, \sigma[\delta\, u_k] = 0$ on $\mathcal{O}$ and $\sigma[\delta\, u_k]\nu = \delta \sigma_k \nu$ on $\mathcal{S}$. $\square$

The first Piola–Kirchhoff stress tensor $\sigma[\delta\, u_k]$ reflects an average of all stresses:

$$\begin{aligned}
&\sigma[\delta\, u_k]\, \mathrm{cof}\mathcal{D}(\mathbb{1}+\delta u_k)\\
&= \left(\frac{1}{n}\sum_{i=1}^{n} W_{,A}(\mathcal{D}((\mathbb{1}+\delta u_k)\circ\phi_i))\, \mathrm{cof}\mathcal{D}((\mathbb{1}+\delta u_k)\circ\phi_i)\right)\circ\phi_i^{-1}\\
&= \left(\frac{1}{n}\sum_{i=1}^{n}\sigma_i[\delta\, u_k]\right)\circ(\mathbb{1}+\delta u_k)\,,
\end{aligned}$$

where the $\sigma_i[\delta\, u_k]$ are indeed the Cauchy stresses of the different objects $\mathcal{O}_i$ when deformed into $(\mathbb{1}+\delta u_k)(\mathcal{O}) = ((\mathbb{1}+\delta u_k)\circ\phi_i)(\mathcal{O}_i)$.

5.2 Remark. *The boundary integral $\int_{\mathcal{S}}\sigma_k\nu\cdot\psi\, da$ can be replaced by the volume integral $\int_{\mathcal{O}}\sigma_k : \mathcal{D}\psi\,\mathrm{d}x \longleftrightarrow$ numerically more convenient.*

shortcoming: As long as $A \mapsto W(A)$ is not quadratic in A, u_k still solves a nonlinear elastic problem.

alternative: consider the limit $\delta \to 0$ of the Euler–Lagrange equations

5.3 Lemma. *In the limit for $\delta \to 0$ an infinitesimal variation u_k of the average shape $\mathcal{S}$ uniquely solves*

$$\textit{div}\,(\mathbf{C}\,\epsilon[u]) = 0 \textit{ in } \mathcal{O}\,, \quad \mathbf{C}\,\epsilon[u]\,\nu = \sigma_k \nu \textit{ on } \mathcal{S}$$

under the constraints $\int_{\mathcal{O}} u\,\mathrm{d}x = 0$ and $\int_{\mathcal{O}} x \times u\,\mathrm{d}x = 0$ where $\mathbf{C}$ is the compound elasticity tensor:

$$\mathbf{C} = \frac{1}{n}\sum_{i=1}^{n}\left(\frac{1}{\det \mathcal{D}\phi_i}\mathcal{D}\phi_i W_{,AA}[\mathcal{D}\phi_i]\mathcal{D}\phi_i^{\mathrm{T}}\right)\circ \phi_i^{-1}$$

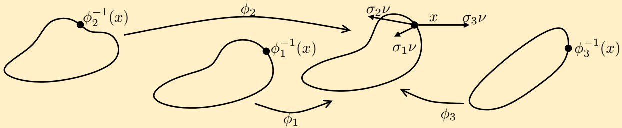

Linearization based on infinitesimal variations (cont.)

Proof. linearization for small δ yields

$$
\begin{aligned}
\mathcal{E}_k[\delta,u] \;\doteq\;& \frac{1}{n}\sum_{i=1}^{n}\Big(\mathcal{W}[\mathcal{O}_i,\phi_i] + \delta\int_{\mathcal{O}_i} W_{,A}[\mathcal{D}\phi_i] : \mathcal{D}(u\circ\phi_i)\,\mathrm{d}x \\
&+\frac{\delta^2}{2}\int_{\mathcal{O}_i} W_{,AA}[\mathcal{D}\phi_i]\mathcal{D}(u\circ\phi_i) : \mathcal{D}(u\circ\phi_i)\,\mathrm{d}x\Big) - \delta^2\int_{\mathcal{O}}\sigma_k : \mathcal{D}u\,\mathrm{d}x \\
=\;& C + \delta\int_{\mathcal{S}}\left(\frac{1}{n}\sum_{i=1}^{n}\sigma_i\nu\right)\cdot u\,\mathrm{d}a - \delta\int_{\mathcal{O}}\left(\frac{1}{n}\sum_{i=1}^{n}\mathrm{div}\,\sigma_i\right)\cdot u\,\mathrm{d}x \\
&\frac{\delta^2}{2n}\sum_{i=1}^{n}\int_{\mathcal{O}}\left(\frac{\mathcal{D}\phi_i W_{,AA}[\mathcal{D}\phi_i]\mathcal{D}\phi_i^{\mathrm{T}}}{\det\mathcal{D}\phi_i}\right)\circ\phi_i^{-1}\mathcal{D}u : \mathcal{D}u\,\mathrm{d}x - \delta^2\int_{\mathcal{O}}\sigma_k : \mathcal{D}u\,\mathrm{d}x \\
=\;& C + \delta^2\int_{\mathcal{O}}\frac{1}{2}\mathbf{C}\mathcal{D}u : \mathcal{D}u - \sigma_k : \mathcal{D}u\,\mathrm{d}x \\
=\;& C + \delta^2\int_{\mathcal{O}}\frac{1}{2}\mathbf{C}\epsilon[u] : \epsilon[u] - \sigma_k : \mathcal{D}u\,\mathrm{d}x.
\end{aligned}
$$

for $\mathbf{C} = \frac{1}{n}\sum_{i=1}^{n}\left(\frac{1}{\det\mathcal{D}\phi_i}\mathcal{D}\phi_i W_{,AA}[\mathcal{D}\phi_i]\mathcal{D}\phi_i^{\mathrm{T}}\right)\circ\phi_i^{-1}$

$\square$

$$\mathbf{C} = \frac{1}{n}\sum_{i=1}^n \left(\frac{1}{\det \mathcal{D}\phi_i} \mathcal{D}\phi_i W_{,AA}[\mathcal{D}\phi_i] \mathcal{D}\phi_i^{\mathrm{T}} \right) \circ \phi_i^{-1}$$

Weak form of the problem to be solve:

Find $u_k : \mathcal{O} \to \mathbb{R}^d$, such that

$$\int_{\mathcal{O}} \mathbf{C}\epsilon[u_k] : \epsilon[\psi] - \sigma_k : \mathcal{D}\psi \,\mathrm{d}x = 0$$

for all smooth test functions $\psi : \mathcal{O} \to \mathbb{R}^d$.

numerical implementation: Discretize this with finite elements, where the finite element approximation of the elastic covariance metric is given by

$$\left(\frac{1}{n} \sum_{i=1}^n \int_{\mathcal{O}_i} W_{,AA}[\mathcal{D}\Phi_i] \mathcal{D}(\Theta_j \circ \Phi_i\, e_r) : \mathcal{D}(\Theta_k \circ \Phi_i\, e_s) \,\mathrm{d}x \right)_{ikrs},$$

where $\Theta_j\, e_r$, $\Theta_k\, e_s$ represent the vector-valued finite element basis functions.

- General set up
- Linear shape variations
- The actual covariance analysis
- Applications

Recalling the ingredients of a shape PCA

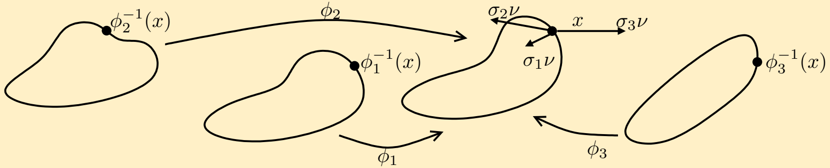

normal stresses $\sigma_k\nu[\mathcal{S}] : \mathcal{S} \to \mathbb{R}^d$ $(k = 1, \ldots, n)$ as shape representations with $0 = \sum_{k=1,\ldots,n} \sigma_k n[\mathcal{S}](x)$

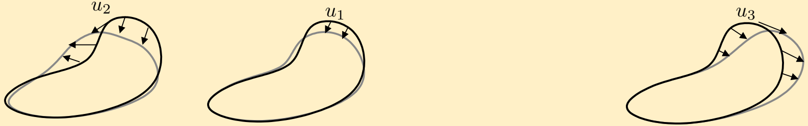

displacements $u_k : \mathcal{O} \to \mathbb{R}^d$, $k = 1, \ldots, n$ with $\sum_{k=1}^n u_k = 0$

$$
\begin{aligned}
\mathrm{div}(\mathbf{C}\epsilon[u_k]) &= 0 && \text{on } \mathcal{O}, \quad \mathbf{C} = \text{elasticity tensor (compound config.)} \\
\mathbf{C}\epsilon[u_k]\nu &= \sigma_k\nu && \text{on } \mathcal{S}
\end{aligned}
$$

Outline of the principal component analysis

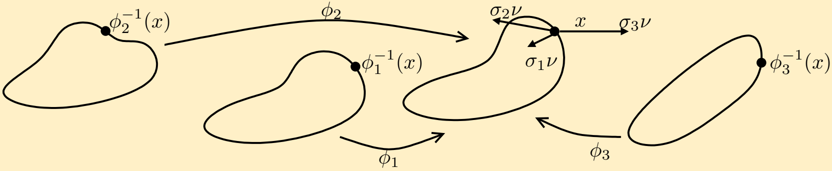

Covariance metric: inner product $\mathbf{g}(\sigma_1\nu, \sigma_2\nu) := g(u_1, u_2)$

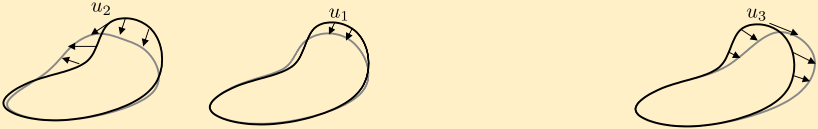

input data	$X = (u_1 \vert \dots \vert u_n)$
covariance matrix	$C = (\frac{1}{n} g(u_i, u_j))_{ij}$
matrix decomposition	$C = O \Lambda O^{\mathrm{T}}$
modes of variation	$Y = X O \sqrt{\Lambda^{-1}}$

Two different scalar products on shape variations

- *The L^2-product.* Given two square integrable displacements u, $\tilde{u}$ we define

$$g(u,v) := \int_{\mathcal{O}} u \cdot v \,\mathrm{d}x$$

This product weights local displacements equally on the whole compound object $\mathcal{O}$.

- *The Hessian of the energy as inner product.*

$$g(u,v) := \int_{\mathcal{O}} \mathbf{C}\epsilon[u] : \epsilon[v] \,\mathrm{d}x$$

This product weights local displacements higher in heavily prestressed areas of the compound object $\mathcal{O}$.

5.4 Remark. *That g induces a metric*

$$\tilde{g}(\sigma\nu, \tilde{\sigma}\nu) := g(u, \tilde{u})$$

on the associated boundary stress.

Due to the linearity of the operator $\sigma\nu \mapsto u$ the metric $\tilde{g}$ is bilinear and symmetric as well.

Finally, the positive definiteness of $\tilde{g}$ follows from the positive definiteness of g and the injectivity of the map $\sigma\nu \mapsto u$.

- General set up
- Linear shape variations
- The actual covariance analysis
- Applications

Qualitative properties

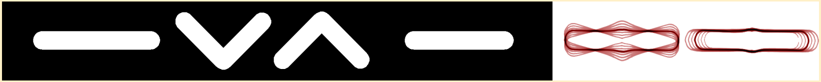

Two dominant modes (right) for four different shapes (left) demonstrate that our principal component analysis properly captures strong geometric nonlinearities.

Average and variation (right) for two shapes with pins at different positions (left). The pins are not interpreted as shifted versions of each other.

Qualitative properties (cont.)

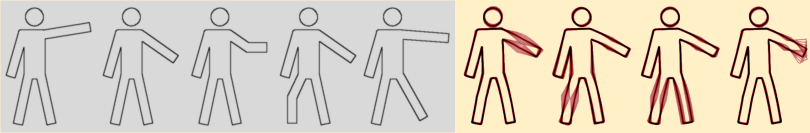

A set of input shapes and their modes of variation with ratios $\frac{\lambda_i}{\lambda_1}$ of 1, 0.22, 0.15, and 0.06.

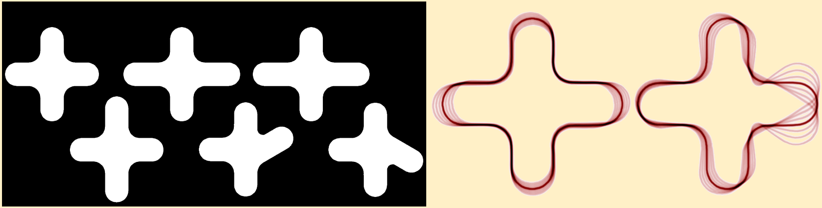

Six input shapes and their first two modes of variation with ratios $\frac{\lambda_i}{\lambda_1}$ of 1 and 0.34.

Dependance on the chosen scalar product

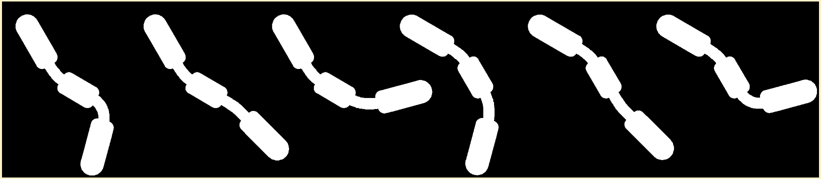

- $g(u,v) := (u,v)_{L^2}$
  with $\mathcal{O}$ non-prestressed

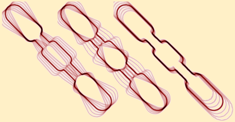

- $g(u,v) := (u,v)_{L^2}$
  with $\mathcal{O}$ prestressed

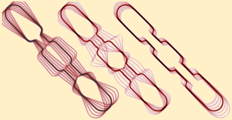

- $g(u,v) := \int_{\mathcal{O}} \mathbf{C}\epsilon[u] : \epsilon[v]\,\mathrm{d}x$
  with $\mathcal{O}$ prestressed

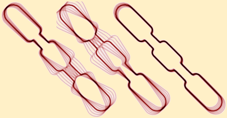

First three modes of variation with ratios $\frac{\lambda_i}{\lambda_1}$ of 1, 0.49, and 0.26 for 8 fish silhouettes (shape database Centre for Vision, Speech, and Signal Processing, University of Surrey)

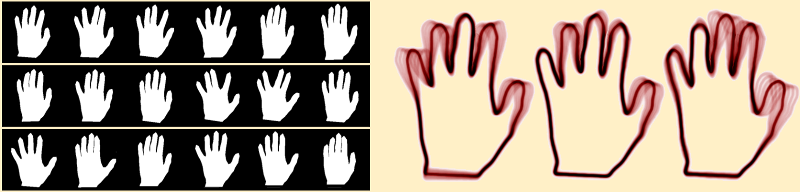

First three modes of variation with ratios $\frac{\lambda_i}{\lambda_1}$ of 1, 0.88, and 0.42 for 18 hand silhouettes from [Cootes, Tayler, Cooper, Graham '95]

"device7" from MPEG7 database

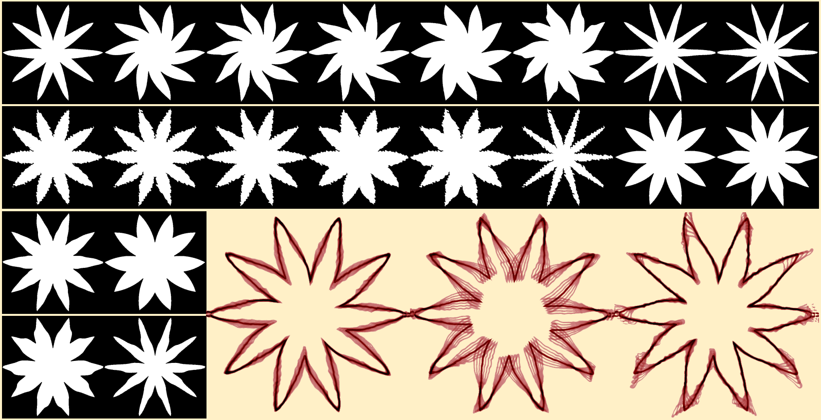

Role of elasticity model

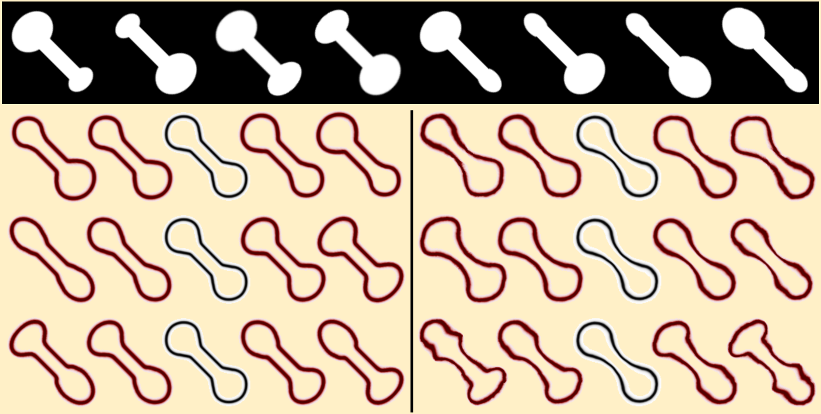

high length change penalization | high volume change penalization

Application to image morphologies

covariance analysis based on the scalar product $g(u,v) = \int_{\mathcal{O}} u \cdot v \, \mathrm{d}x$

Variation of segmented kidneys

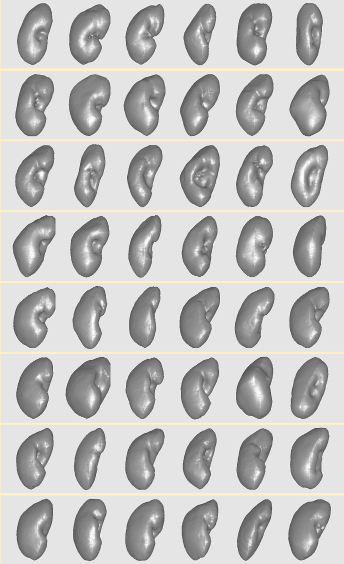

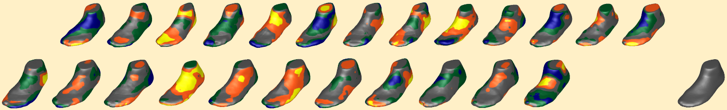

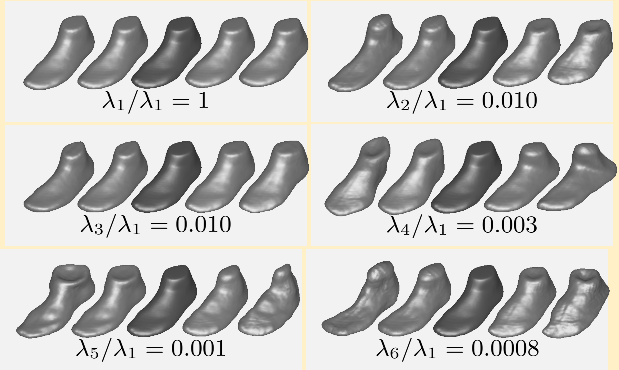

covariance analysis for scalar product $g(u,v) = \int_{\mathcal{O}} u \cdot v \,\mathrm{d}x$

Variation of foot scans (cont.)

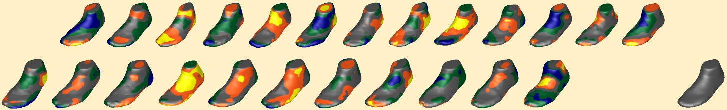

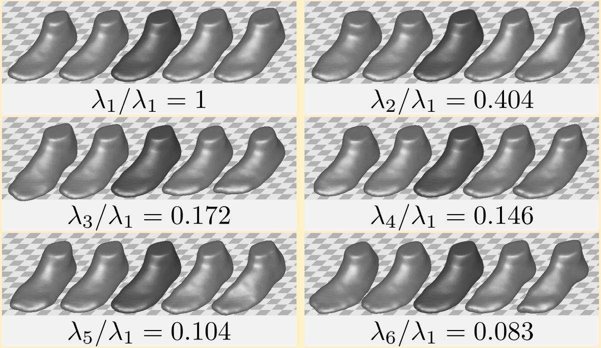

covariance analysis for scalar product $g(u,v) = \int_{\mathcal{O}} C\epsilon[u] : \epsilon[v]\,\mathrm{d}x$

modes representing change in volume (λ_1), width / length (λ_2) variation of toe positions (λ_3, λ_4) and heel position / instep shape (λ_5, λ_6)

Using the PCA to analyze additional feet

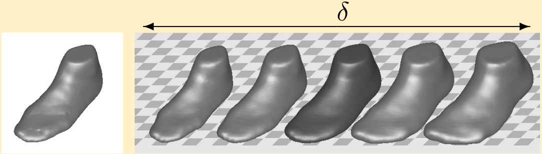

For a new, additional foot (top left), a linear representative $\hat{u}$ is computed and visualized as a variation of the average foot $\mathcal{S}$ via $(\mathbb{1} + \delta\hat{u})(\mathcal{S})$ (top right)

Mahalanobis distance $d_M(\hat{\mathcal{S}}, \mathcal{S}) = \sqrt{\frac{1}{n}\sum_{k=1}^{n} \frac{g(\hat{u}, y_k)^2}{\lambda_k}} = 1.23$

($d_M = 1$ would correspond to the standard deviation)

reconstruction using modes

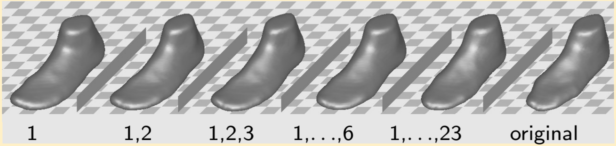

using PCA to reconstruct the new foot

- Time discrete geodesic paths
- A relaxed formulation
- The numerical algorithm
- Limit of the time discrete model
- Qualitative properties of the model
- Generalized models

- Time discrete geodesic paths
- A relaxed formulation
- The numerical algorithm
- Limit of the time discrete model
- Qualitative properties of the model
- Generalized models

Recalling the definition of a geodesic

- The metric $\mathcal{G}$ on the (infinite-dimensional) manifold $\mathbf{S}$ assigns each element $\mathcal{S} \in \mathbf{S}$ an inner product on variations $\delta\mathcal{S}$ of $\mathcal{S}$.
- The metric is based on physical dissipation in a viscous fluid model:

$$\mathcal{G}(\delta S, \delta S) := \min_{v \in \mathcal{V}(\delta\mathcal{S})} \int_{\mathcal{O}} \mathbf{diss}[v] \, \mathrm{d}x$$

- A geodesic path between $\mathcal{S}_A$ and $\mathcal{S}_B$ in $\mathbf{S}$ is a curve $(\mathcal{S}(t))_{t\in[0,1]} \subset \mathbf{S}$ with $\mathcal{S}(0) = \mathcal{S}_A$ and $\mathcal{S}(1) = \mathcal{S}_B$, which (locally) minimizes

$$\mathbf{Diss}\left[(v(t), \mathcal{O}(t))_{t\in[0,1]}\right] = \int_0^1 \mathcal{G}(\dot{S}(t), \dot{S}(t)) \, \mathrm{d}t$$

among all differentiable paths in $\mathbf{S}$ and all consistent motion fields $v(t) \in \mathcal{V}(\dot{\mathcal{S}}(t))$.

An approximate time discrete geodesic between s_A and s_B:

Consider points $s_A = s_0, s_1, \ldots, s_K = s_B$ and minimize

$$\frac{1}{\tau} \sum_{k=1}^{K} \mathrm{dist}^2(s_{k-1}, s_k) \quad \left(\approx \int_0^1 g(\dot{s}, \dot{s}) \, \mathrm{d}t \right),$$

where $\mathrm{dist}(\cdot, \cdot)$ is an approximate Riemannian distance and $\tau = \frac{1}{K}$.

example: spherical projection onto $\mathbb{R}^2$

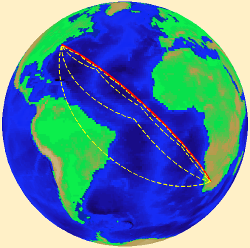

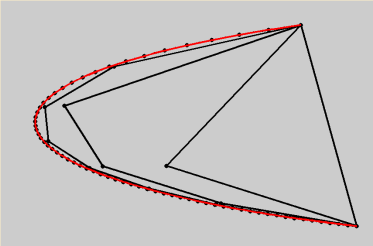

aim: infinite-dimensional counterpart in shape space

Goals of this approach

- a physically sound modeling of the geodesic flow of shapes given as boundary contours of objects on a void background
- a coarse time discretization which is nevertheless invariant with respect to rigid body motions and ensures a 1-1 object correspondence
- approximation of a continuous geodesic path for decreasing time step
- a numerically effective hierarchical treatment of the resulting problem in space time

consider for given shapes $\mathcal{S}_A$, $\mathcal{S}_B$ in a shape space $\mathbf{S}$

discrete path of shapes

sequence $\mathcal{S}_0, \mathcal{S}_1, \ldots, \mathcal{S}_K$ of shapes with $\mathcal{S}_0 = S_A$, $\mathcal{S}_K = S_B$,
where $\mathcal{S}_k$ approximates $\mathcal{S}(t_k)$ on a continuous path $\mathcal{S}(t)$

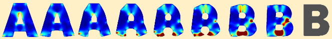

matching deformation

deformation ϕ_k for each pair $\mathcal{S}_{k-1}, \mathcal{S}_k$ with $\phi_k(\mathcal{S}_{k-1}) = \mathcal{S}_k$
associated with a deformation energy

$$\mathcal{W}[\phi_k, \mathcal{S}_{k-1}] = \int_{\mathcal{O}_{k-1}} W(\mathcal{D}\phi_k)\,\mathrm{d}x$$

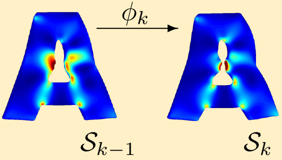

desired properties of $\mathcal{W}[\phi_k, \mathcal{S}_{k-1}] = \int_{\mathcal{O}_{k-1}} W(\mathcal{D}\phi_k)\,\mathrm{d}x$:

- invariance with respect to rigid body motions, i. e.

$$\mathcal{W}[Q\circ\phi_k + b, \mathcal{S}_{k-1}] = \mathcal{W}[\phi_k, \mathcal{S}_{k-1}] \quad \forall Q \in SO(d), b \in \mathbb{R}^d$$

$\Rightarrow W(\mathcal{D}\phi) = \bar{W}(\mathcal{D}\phi^{\mathrm{T}}\mathcal{D}\phi)$ for some $\bar{W}$

- isotropy $\Rightarrow \bar{W}(\mathcal{D}\phi^{\mathrm{T}}\mathcal{D}\phi) = \hat{W}(\mathcal{D}\phi, \mathrm{cof}\mathcal{D}\phi, \det\mathcal{D}\phi)$

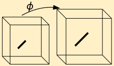

$\mathrm{tr}(\mathcal{D}\phi^{\mathrm{T}}\mathcal{D}\phi)$

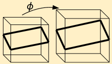

$\mathrm{tr}(\mathrm{cof}(\mathcal{D}\phi^{\mathrm{T}}\mathcal{D}\phi))$

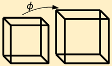

$\det(\mathcal{D}\phi^{\mathrm{T}}\mathcal{D}\phi)$

with $\hat{W}$ convex in $\mathcal{D}\phi$, $\mathrm{cof}\mathcal{D}\phi$, $\det\mathcal{D}\phi$ (polyconvexity)
and ensuring injectivity of ϕ under certain growth conditions

- isometries ($\mathcal{D}\phi^{\mathrm{T}}(x)\mathcal{D}\phi(x) = \mathrm{id}$) are minimizers, $\bar{W}(\mathrm{id}) = 0$.

In what follows, we again choose

$$\hat{W}(A, C, D) = a_1|A|^p + a_2|C|^q + \Gamma(D)$$

6.1 Definition (Discrete dissipation and discrete path length). *Given a discrete path $\mathcal{S}_0, \mathcal{S}_1, \ldots, \mathcal{S}_K \in \mathbf{S}$, the total dissipation along a path can be computed as*

$$\mathbf{Diss}_\tau(\mathcal{S}_0, \mathcal{S}_1, \ldots, \mathcal{S}_K) := \sum_{k=1}^{K} \frac{1}{\tau} \mathcal{W}[\phi_k, \mathcal{S}_{k-1}],$$

where ϕ_k is a minimizer of the deformation energy $\mathcal{W}[\cdot, \mathcal{S}_{k-1}]$ over $\mathbf{D}[\mathcal{O}_{k-1}]$ under the constraint $\phi_k(\mathcal{S}_{k-1}) = \mathcal{S}_k$. Furthermore, the discrete path length is defined as

$$L_\tau(\mathcal{S}_0, \mathcal{S}_1, \ldots, \mathcal{S}_K) := \sum_{k=1}^{K} \sqrt{\mathcal{W}[\phi_k, \mathcal{S}_{k-1}]}\,.$$

Here $\mathbf{D}[\mathcal{O}_{k-1}]$ is a space of admissible deformations on $\mathcal{O}_{k-1}$.

6.2 Definition (discrete geodesic path). *A discrete path $\mathcal{S}_0, \mathcal{S}_1, \ldots, \mathcal{S}_K$ in a set of admissible shapes $\mathbf{S}$ connecting two shapes $\mathcal{S}_A$ and $\mathcal{S}_B$ in $\mathbf{S}$ is a discrete geodesic if there exists an associated family of deformations $(\phi_k)_{k=1,\ldots,K}$ with $\phi_k \in \mathbf{D}[\mathcal{O}_{k-1}]$ and $\phi_k(\mathcal{S}_{k-1}) = \mathcal{S}_k$ such that $(\phi_k, \mathcal{S}_k)_{k=1,\ldots,K}$ minimize the total energy $\sum_{k=1}^{K} \mathcal{W}[\tilde{\phi}_k, \tilde{\mathcal{S}}_{k-1}]$ over all intermediate shapes $\tilde{\mathcal{S}}_1, \ldots, \tilde{\mathcal{S}}_{K-1} \in \mathbf{S}$ and all possible matching deformations $\tilde{\phi}_1, \ldots, \tilde{\phi}_K$ with $\tilde{\phi}_k \in \mathbf{D}[\tilde{\mathcal{O}}_{k-1}]$, $\tilde{\mathcal{S}}_{k-1} = \partial\tilde{\mathcal{O}}_{k-1}$, and $\tilde{\phi}_k(\tilde{\mathcal{S}}_{k-1}) = \tilde{\mathcal{S}}_k$ for $k = 1, \ldots, K$.*

In case $d = 3$ with

$$\hat{W}(A, C, D) = a_1|A|^p + a_2|C|^q + a_3\left(D^{-s} + \beta D^r\right) - \gamma$$

with $a_1, a_2, a_3, \beta, \gamma > 0$, $p, q > 3$, $r > 1$ and $s > \frac{2q}{q-3}$ choose

$$\begin{aligned}\mathbf{D}[\mathcal{O}_{k-1}] := \; & \{\phi : \mathcal{O}_{k-1} \to \mathbb{R}^d \;\big|\; \phi \in W^{1,p}(\mathcal{O}_{k-1}), \mathrm{cof}\mathcal{D}\phi \in L^q(\mathcal{O}_{k-1}), \\ & \det \mathcal{D}\phi \in L^r(\mathcal{O}_{k-1}), \det \mathcal{D}\phi > 0 \text{ a.e. in } \mathcal{O}_{k-1}, \phi(\mathcal{O}_{k-1}) = \mathcal{O}_k\}\,.\end{aligned}$$

6.3 Theorem (Existence of a discrete geodesic). *If $\mathbf{S}$ consists of shapes $\mathcal{S}$ which are boundary contours of open, bounded sets $\mathcal{O}$ and can be decomposed into a bounded number of spline surfaces with control points on a fixed compact domain. Furthermore, the shapes are supposed to fulfill a two-sided uniform cone condition. Given two diffeomorphic shapes $\mathcal{S}_A$ and $\mathcal{S}_B$ in the above shape space $\mathbf{S}$, there exists a discrete geodesic $\mathcal{S}_0, \mathcal{S}_1, \ldots, \mathcal{S}_K \in \mathbf{S}$ connecting $\mathcal{S}_A$ and $\mathcal{S}_B$. The associated deformations $\phi_1, \ldots, \phi_K$ with $\phi_k \in \mathbf{D}[\mathcal{O}_{k-1}]$ for $k = 1, \ldots, K$ are Hölder continuous and locally injective in the sense that the determinant of the deformation gradient is positive almost everywhere.*

Proof.

• Applying classical existence theory in nonlinear elasticity [Ball '77] there exists for any (fixed) pair of consecutive shapes $\mathcal{S}_{k-1}$ and $\mathcal{S}_k$ a minimizing deformation $\phi_k \in \mathbf{D}[\mathcal{O}_{k-1}]$ with $\det \mathcal{D}\phi_k > 0$ almost everywhere, which minimizes $\mathcal{W}[\cdot, \mathcal{S}_{k-1}]$. Hence, the discrete dissipation is well–defined.

• The shape space $\mathbf{S}$ can be parametrized with finitely many parameters, namely the control points of the spline segments. These control points lie in a compact set and $\mathbf{S}$ is closed with respect to the convergence of these parameters.

• Hence, it is sufficient to verify that $\mathbf{Diss}_\tau$ is continuous function of the finite set of spline parameters. Consider shapes $\mathcal{S}_{k-1}$, $\mathcal{S}_k$ and $\tilde{\mathcal{S}}_{k-1}$, $\tilde{\mathcal{S}}_k$, respectively.

For a given small $\delta_0 \geq \delta > 0$ assume that the spline parameters are closed, such that there exists bijective deformations $\psi_i : \tilde{\mathcal{O}}_i \to \mathcal{O}_i$ with

$$\left|\psi_i - \mathbb{1}\right|_{1,\infty} + \left|\psi_i^{-1} - \mathbb{1}\right|_{1,\infty} \leq \delta\,.$$

- Now define $\hat{\phi} := \psi_k^{-1} \circ \phi \circ \psi_{k-1}$ and estimate

$$
\begin{aligned}
\mathbf{Diss}_\tau(\tilde{\mathcal{S}}_{k-1}, \tilde{\mathcal{S}}_k) - \mathbf{Diss}_\tau(\mathcal{S}_{k-1}, \mathcal{S}_k) &= \frac{1}{\tau} \int_{\tilde{\mathcal{O}}_{k-1}} W(\mathcal{D}\tilde{\phi})\,\mathrm{d}x - \frac{1}{\tau} \int_{\mathcal{O}_{k-1}} W(\mathcal{D}\phi)\,\mathrm{d}x \\
&\le \frac{1}{\tau} \int_{\tilde{\mathcal{O}}_{k-1}} W(\mathcal{D}\hat{\phi})\,\mathrm{d}x - \frac{1}{\tau} \int_{\mathcal{O}_{k-1}} W(\mathcal{D}\phi)\,\mathrm{d}x \\
&= \frac{1}{\tau} \int_{\mathcal{O}_{k-1}} W\big((\mathcal{D}\psi_k^{-1} \circ \phi)\mathcal{D}\phi(\mathcal{D}\psi_{k-1} \circ \psi_{k-1}^{-1})\big)\,|\det \mathcal{D}\psi_{k-1}^{-1}| - W(\mathcal{D}\phi)\,\mathrm{d}x \\
&\le \frac{c(\delta_0)}{\tau} \int_{\mathcal{O}_{k-1}} |\mathcal{D}\phi|^p + |\mathrm{cof}\mathcal{D}\phi|^q + |\det \mathcal{D}\phi|^r + \left|(\det \mathcal{D}\phi)^{-1}\right|^s\,\mathrm{d}x
\end{aligned}
$$

Hence, due to the Lebesgue's convergence theorem we obtain convergence

$$
\lim_{\delta \to 0} \mathbf{Diss}_\tau(\tilde{\mathcal{S}}_{k-1}, \tilde{\mathcal{S}}_k) - \mathbf{Diss}_\tau(\mathcal{S}_{k-1}, \mathcal{S}_k) \le 0
$$

□

The hard constraint model (cont.)

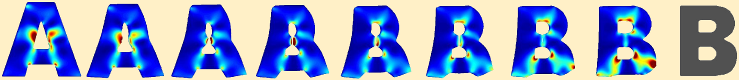

geodesic path ($L = 0.2225$, $\mathbf{Diss} = 0.0497$)

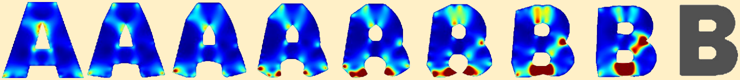

non geodesic path ($L = 0.2886$, $\mathbf{Diss} = 0.0880$)

Time discrete geodesic

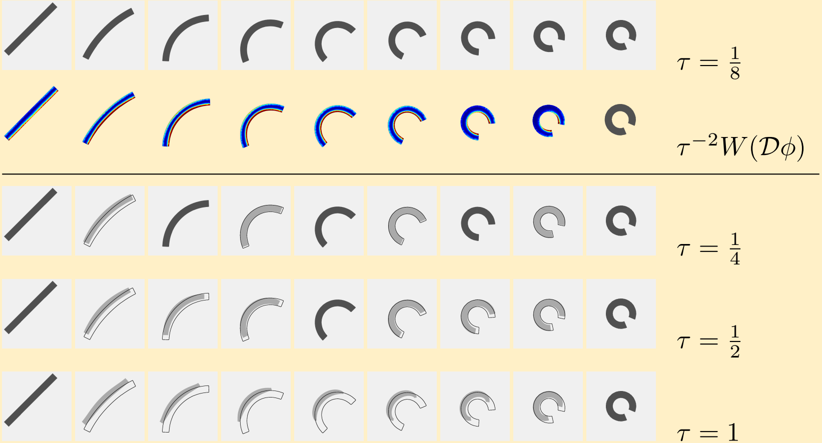

based on a relaxed formulation

- Time discrete geodesic paths
- A relaxed formulation
- The numerical algorithm
- Limit of the time discrete model
- Generalized models

- Soft material outside $\mathcal{O}_{k-1}$ $(0 < \delta << 1)$

$$\mathcal{W}^\delta[\phi_k, \mathcal{S}_{k-1}] = \int_\Omega \Big((1-\delta)\chi_{\mathcal{O}_{k-1}} + \delta\Big) W(\mathcal{D}\phi_k)\,\mathrm{d}x$$

- Replace hard constraint $\phi_k(\mathcal{S}_{k-1}) = \mathcal{S}_k$ by the mismatch penalty (ϕ_k extended outside $\mathcal{O}_{k-1}$)

$$\mathcal{F}[\phi_k, \mathcal{S}_{k-1}, \mathcal{S}_k] = \mathrm{vol}(\mathcal{O}_{k-1} \triangle \phi_k^{-1}(\mathcal{O}_k))\,,$$

where $A \triangle B = A \setminus B \cup B \setminus A$

- additional regularizing surface energy $\mathcal{L}[\mathcal{S}] = \int_{\mathcal{S}} \mathrm{d}a$

Relaxed formulation

$$\mathcal{E}_\tau^\delta[(\phi_k, \mathcal{S}_{k-1}, \mathcal{S}_k)_{k=1,\ldots,K}] = \sum_{i=1}^{K} \Big(\frac{1}{\tau}\mathcal{W}^\delta[\phi_k, \mathcal{S}_{k-1}] + \gamma\mathcal{F}[\phi_k, \mathcal{S}_{k-1}, \mathcal{S}_k] + \mu\tau\mathcal{L}[\mathcal{S}_k]\Big)$$

Describing shapes via level sets:

$$\mathcal{O}(t) = \{x \in \Omega \,:\, u(t,x) > 0\}$$

Encode partition into object and background via regularized Heaviside function $H_\epsilon(x) := \frac{1}{2} + \frac{1}{\pi}\arctan\left(\frac{x}{\epsilon}\right)$ [Chan, Vese '01]

$$\begin{aligned}
\mathcal{E}^{\epsilon}_{\text{match}}[\phi_k, u_{k-1}, u_k] &= \int_\Omega \left(H_\epsilon(u_k(\phi_k)) - H_\epsilon(u_{k-1})\right)^2 \,\mathrm{d}x \\
\mathcal{E}^{\epsilon}_{\text{area}}[u_k] &= \int_\Omega |\nabla H_\epsilon(u_k)| \,\mathrm{d}x \\
\mathcal{E}^{\epsilon,\delta}_{\text{deform}}[\phi_k, u_{k-1}] &= \int_\Omega \left((1-\delta)H_\epsilon(u_{k-1}) + \delta\right) W(\mathcal{D}\phi_k) \,\mathrm{d}x,
\end{aligned}$$

(here $\delta = 10^{-4}$)

$$\mathcal{E}^{\varepsilon,\delta}_{\tau}[(\phi_k, u_k)_k] = \sum_{k=1}^{K} \frac{1}{\tau}\mathcal{E}^{\varepsilon,\delta}_{\text{deform}}[\phi_k, u_{k-1}] + \eta\mathcal{E}^{\varepsilon}_{\text{match}}[\phi_k, u_{k-1}, u_k] + \mu\tau\mathcal{E}^{\varepsilon}_{\text{area}}[u_k]$$

- Time discrete geodesic paths
- A relaxed formulation
- The numerical algorithm
- Limit of the time discrete model
- Qualitative properties of the model
- Generalized models

Cascadic finite elements discretization

- multilinear finite elements, regular quadrilateral grid, $\Omega = [0,1]^d$
- Gaussian quadrature of third order on each grid cell
- pushforwards $U \circ \Phi$ evaluated exactly at quadrature points (for discretized level set functions and deformations U, Φ)
- alternating gradient descent steps
  - all deformations
  - all level set functions
- Armijo stepsize control
- dyadic grid resolution: $2^L + 1$ vertices in each direction
- multi-level approach:
  - initial optimization on a coarse scale
  - successive refinement
  - interface parameter linked to grid size: $\epsilon = h$

A sketch of the algorithm

EnergyRelaxation $(U_{\mathrm{start}}, U_{\mathrm{end}})$
for time level $j = j_0$ to J {
$K = 2^j$; $U_0^j = U_{\mathrm{start}}$; $U_K^j = U_{\mathrm{end}}$
if $(j = j_0)$ {
initialize $\Phi_i^j = \mathbb{1}$, $U_i^j = U_K^j$, $i = 1, \ldots, K$
} **else** {
initialize $\Phi_{2i-1}^j = \mathbb{1} + \frac{1}{2}(\Phi_i^{j-1} - \mathbb{1})$, $\Phi_{2i}^j = \Phi_i^{j-1} \circ (\Phi_{2i-1}^j)^{-1}$,
$U_{2i}^j = U_i^{j-1}$, $U_{2i-1}^j = U_i^{j-1} \circ \Phi_{2i}^j$, $i = 1, \ldots, \frac{K}{2}$ }
restrict $\mathbf{U}_i^j$, $\mathbf{\Phi}_i^j$ for all $i = 1, \ldots, K$ onto the coarsest grid level l_0;
for grid level $l = l_0$ to L {
for step $k = 0$ to $k_{\max}$ {
$(\mathbf{\Phi}_i)_{i=1,\ldots,K} = (\mathbf{\Phi}_i^{\mathrm{old}})_{i=1,\ldots,K} - \tau \, \mathrm{grad}_{(\mathbf{\Phi}_i^{\mathrm{old}})_{i=1,\ldots,K}} \mathcal{E}_\tau^{\varepsilon,\delta}[(\mathbf{U}_i, \mathbf{\Phi}_i)_{i=1,\ldots,K}]$
$(\mathbf{U}_i)_{i=1,\ldots,K} = (\mathbf{U}_i^{\mathrm{old}})_{i=1,\ldots,K} - \tau \, \mathrm{grad}_{(\mathbf{U}_i^{\mathrm{old}})_{i=1,\ldots,K}} \mathcal{E}_\tau^{\varepsilon,\delta}[(\mathbf{U}_i, \mathbf{\Phi}_i)_{i=1,\ldots,K}]$
with Armijo step size control for τ;
}
if $(l < L)$ prolongate $\mathbf{U}_i^j$, $\mathbf{\Phi}_i^j$ for all $i = 1, \ldots, K$ onto the next grid level;
}
}

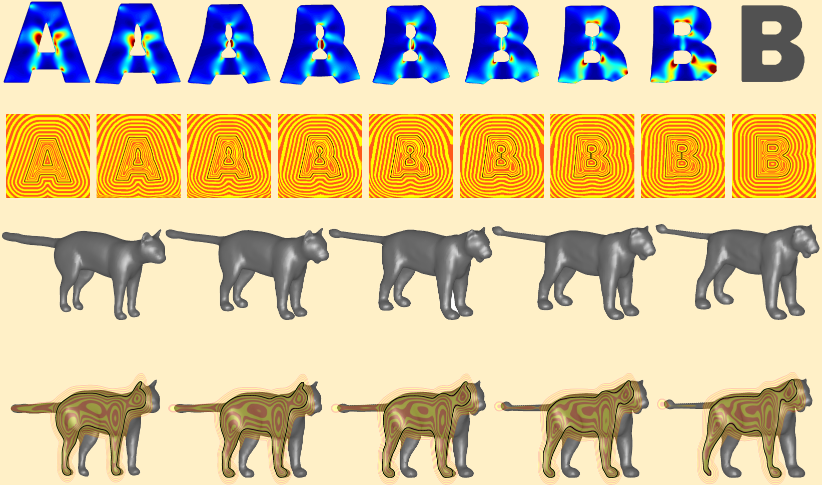

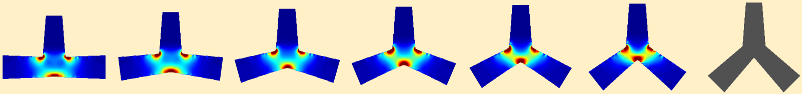

cf. [Charpiat, Faugeras, Keriven '05]

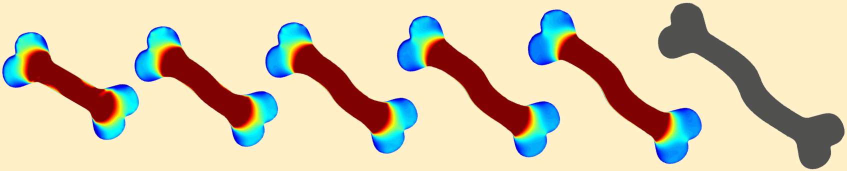

cf. [Fuchs, Jüttler, Scherzer, Yang '09]

Continuity with respect to shape variations:

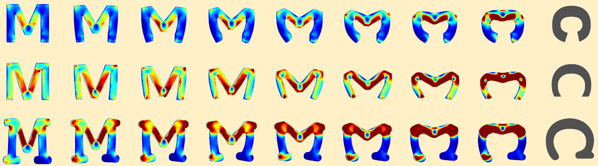

$L = 0.1040$

$L = 0.1220$

$L = 0.1276$

Evaluating the lack of symmetry:

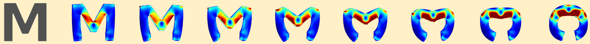

$L = 0.1030$

Geodesic distances for discrete geodesics of different resolutions:

	$K=4$	$K=8$	$K=16$
	0.1068	0.1040	0.1025
	0.1265	0.1220	0.1201
	0.1324	0.1276	0.1259

- Time discrete geodesic paths
- A relaxed formulation
- The numerical algorithm
- Limit of the time discrete model
- Qualitative properties of the model
- Generalized models

Recall:

$$
\begin{aligned}
\mathbf{diss}[v] &= \frac{\lambda}{2}(\mathrm{tr}\epsilon[v])^2 + \mu\mathrm{tr}(\epsilon[v]^2) \\
\hat{W}(A,C,D) &= a_1|A|^p + a_2|C|^q + \Gamma(D)
\end{aligned}
$$

Key assumption:

$$
\mathrm{Hess}\,\mathcal{W}[\mathbb{1},\mathcal{S}](v,v) = 2\int_{\mathcal{O}} \mathbf{diss}[v]\,\mathrm{d}x \quad \forall \text{ velocity fields} \quad v
$$

In terms of the energy density W this is expressed by the condition

$$
\frac{1}{2}\frac{\mathrm{d}^2}{\mathrm{d}t^2}W(\mathbb{1}+tA)|_{t=0} = \frac{\lambda}{2}(\mathrm{tr}A)^2 + \frac{\mu}{\mathrm{tr}}\left(\left(A+A^{\mathrm{T}}\right)^2\right) \qquad (*)
$$

6.4 Lemma (W consistent with diss). *For any local dissipation rate* $\mathbf{diss}$ *one can find a nonlinear energy density* $\bar{W}$ *which satisfies* (∗).

Relating the time discrete and the time continuous model (cont.)

Deducing a discrete flow from a family of successive matches:

Define a temporally piecewise constant motion field v_τ^k and a time-continuous deformation field ϕ_τ^k (interpolating between $x \in \mathcal{O}_{k-1}$ and $\phi_k(x) \in \mathcal{O}_k$) by

$$\begin{aligned} v_\tau^k(t) &:= \frac{1}{\tau}(\phi_k - \mathbb{1}) \,, \\ \phi_\tau^k(t) &:= (\mathbb{1} + (t - t_{k-1}) v_\tau^k) \end{aligned}$$

for $t \in [t_{k-1}, t_k)$ with $t_k = k\tau$.

The corresponding Eulerian motion field is

$$v_\tau(t) := v_\tau^k \circ (\phi_\tau^k)^{-1} \,.$$

6.5 Theorem (convergence to the viscous model). *Let* $(\mathcal{S}(t))_{t\in[0,1]}$ *be a smooth family of shapes. Consider* $\mathcal{S}_k = \mathcal{S}(k\tau)$ *for* $\tau = \frac{1}{K}$ *and* $\phi_1, \ldots, \phi_K$ *a set of injective deformations, such that the associated motion field*

$$v_\tau(t) := v_\tau^k \circ (\phi_\tau^k)^{-1}$$

$(t_{k-1} \leq t < t_k)$ *converges to a regular motion field* v *for* $K \to \infty$. *Furthermore suppose that* $\frac{1}{2}\frac{\mathrm{d}^2}{\mathrm{d}t^2} W_{,AA}(\mathbb{1})(\mathcal{D}v) = \mathbf{diss}[v]$.

Then $\mathcal{E}_\tau[(\phi_k, \mathcal{S}_k)_{k=1,\ldots,K}]$ *converges to*

$$\mathcal{E}[(v(t), \mathcal{S}(t))_{t\in[0,1]}] = \mathbf{Diss}[v] + \gamma\, \mathcal{E}_{OF}[v, S] + \mu \int_0^1 \mathcal{L}[\mathcal{S}(t)]\,\mathrm{d}t$$

for $K \to \infty$. *Here*

$$\mathcal{E}_{OF}[v, S] := \int_{\mathcal{T}} \left|(1, v(t))^{\mathrm{T}} \cdot \nu_{\mathcal{S}}(t)\right| \, da$$

where $n_{\mathcal{S}(t)}$ *denotes the space time normal on the shape tube* $\mathcal{T} = \cup_{t\in[0,1]}(t, \mathcal{S}(t))$ *and* $(1, v(t))$ *is the space time motion field.*

Proof. By second order Taylor one obtain

$$
\begin{aligned}
W(\mathcal{D}\phi_k) &= W(\mathbb{1}) + \tau W_{,A}(\mathbb{1})(\mathcal{D}v_\tau^k) + \frac{\tau^2}{2} W_{,AA}(\mathbb{1})(\mathcal{D}v_\tau^k, \mathcal{D}v_\tau^k) + O(\tau^3) \\
&= 0 + 0 + \frac{\tau^2}{2}\frac{\mathrm{d}^2}{\mathrm{d}t^2} W(\mathbb{1} + t\mathcal{D}v_\tau^k)|_{t=0} + O(\tau^3) \\
&= \tau^2 \mathbf{diss}[v_\tau^k] + O(\tau^3)\,.
\end{aligned}
$$

Summing over all deformation energy contributions yields

$$
\lim_{K\to\infty} \sum_{k=1}^K \frac{1}{\tau}\mathcal{W}[\phi_k, \mathcal{S}_{k-1}] = \lim_{K\to\infty}\sum_{k=1}^K \frac{1}{\tau}\int_{\mathcal{O}_{k-1}} W(D\phi_k)\,\mathrm{d}x
$$

$$
= \lim_{K\to\infty}\sum_{k=1}^K \tau \int_{\mathcal{O}_{k-1}} \mathbf{diss}[v_\tau^k]\,\mathrm{d}x = \int_0^1 \int_{\mathcal{O}(t)} \mathbf{diss}[v]\,\mathrm{d}x\,\mathrm{d}t
$$

Furthermore, $\lim\limits_{K\to\infty} \sum_{k=1}^K \tau \mathcal{L}[\mathcal{S}_k] = \int_0^1 \int_{\mathcal{S}(t)}$ d$a\,\mathrm{d}t$.

Viscous fluid model in the limit for $\tau \to 0$ (cont.)

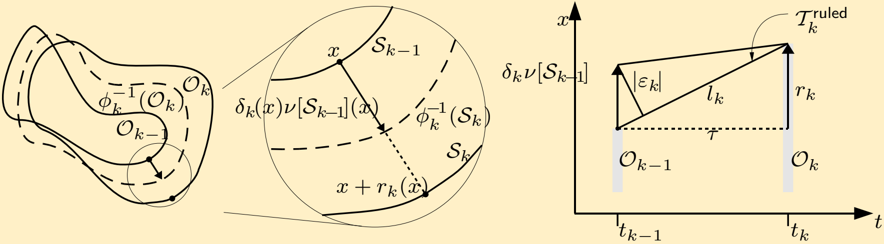

Near $\mathcal{S}_{k-1}$ define $\delta_k(x) := \sup\{s : \phi_k(x + s\nu[\mathcal{S}_{k-1}](x)) \in \mathcal{O}_k\}$.
Furthermore, connect the shapes $\mathcal{S}(t_{k-1})$ and $\mathcal{S}(t_k)$ via a ruled surface

$$\mathcal{T}_k^{\text{ruled}} := \left\{ \left(t, x + \frac{t - t_{k-1}}{\tau} r_k(x) \right) : t \in [t_{k-1}, t_k], x \in \mathcal{S}_{k-1} \right\}$$

approx. the continuous tube $\mathcal{T}_k := \cup_{t_{k-1} \le t \le t_k} (t, \mathcal{S}(t))$ up to $O(\tau^2)$.
For the normal $\nu_k[t_{k-1}, \mathcal{S}_{k-1}]$ on the ruled surface $\mathcal{T}_k^{\text{ruled}}$ we get

$$|(\tau, r_k - \delta_k \nu[\mathcal{S}_{k-1}]) \cdot \nu_k[t_{k-1}, \mathcal{S}_{k-1}]| = \tau \, |(1, v_\tau^k) \cdot \nu_k[t_{k-1}, \mathcal{S}_{k-1}]| + o(\tau) \, .$$

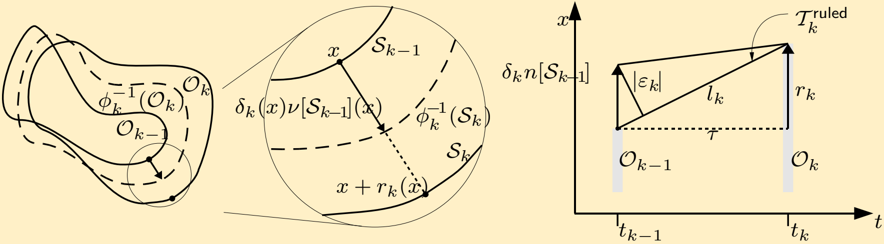

Next, by an elementary geometric argument for $l_k := \sqrt{\tau^2 + |r_k|^2}$ and $\varepsilon_k := (\tau, r_k - \delta_k \nu[\mathcal{S}_{k-1}]) \cdot \nu_k[t_{k-1}, \mathcal{S}_{k-1}]$ one obtains that $\frac{|\varepsilon_k|\, l_k}{\tau} = |\delta_k|$.

$$\int_{\mathcal{T}_k} |(1, v(x)) \cdot \nu[t, \mathcal{S}(t)](x)|\,\mathrm{d}a = \int_{\mathcal{T}_k^{\text{ruled}}} |(1, v_\tau^k(x)) \cdot \nu_k[t_{k-1}, \mathcal{S}_{k-1}](x)|\,\mathrm{d}a + o(\tau)$$

$$= \int_{\mathcal{S}_{k-1}} |(1, v_\tau^k(x)) \cdot \nu_k[t_{k-1}, \mathcal{S}_{k-1}](x)| l_k(x)\,\mathrm{d}a + o(\tau)$$

$$= \int_{\mathcal{S}_{k-1}} \frac{1}{\tau} |(\tau, r_k(x) - \delta_k(x)\nu[\mathcal{S}_{k-1}](x)) \cdot \nu_k[t_{k-1}, \mathcal{S}_{k-1}](x)| l_k(x)\,\mathrm{d}a + o(\tau)$$

$$= \int_{\mathcal{S}_{k-1}} |\delta_k(x)|\,\mathrm{d}a + o(\tau) = \mathrm{vol}(\mathcal{O}_{k-1} \triangle \phi_k^{-1}(\mathcal{O}_k)) + o(\tau) \square$$

$$\mathcal{E}[v,\mathcal{S}] = \mathbf{Diss}[v] + \eta\,\mathcal{E}_{\textsf{OF}}[v,S] + \mu \int_0^1 \mathcal{E}_{\textsf{area}}[\mathcal{S}(t)]\,\mathrm{d}t$$

We can rewrite

$$\begin{aligned}\mathcal{E}_{\textsf{OF}}[(v(t),\mathcal{S}(t))_{t\in[0,1]}] &= \int_{\bigcup_{t\in[0,1]}(t,\mathcal{S}(t))} \left|(1,v(t))^{\mathrm{T}}\cdot \nu_{\mathcal{S}(t)}\right| \,\mathsf{d}a \\ &= \int_{[0,1]\times\mathbb{R}^d} \left|\partial_t \chi_{\mathcal{T}_\mathcal{O}} + \nabla_x \chi_{\mathcal{T}_\mathcal{O}}\cdot v\right| \,\mathrm{d}x\,\mathrm{d}t\,.\end{aligned}$$

where $\mathcal{T}_\mathcal{O} = \bigcup_{t\in[0,1]}(t,\mathcal{O}(t))$.

(cf. TV approaches in optical flow [Black, Anandan '93])

Length versus volume preservation

$\lambda/\mu = 0.01$

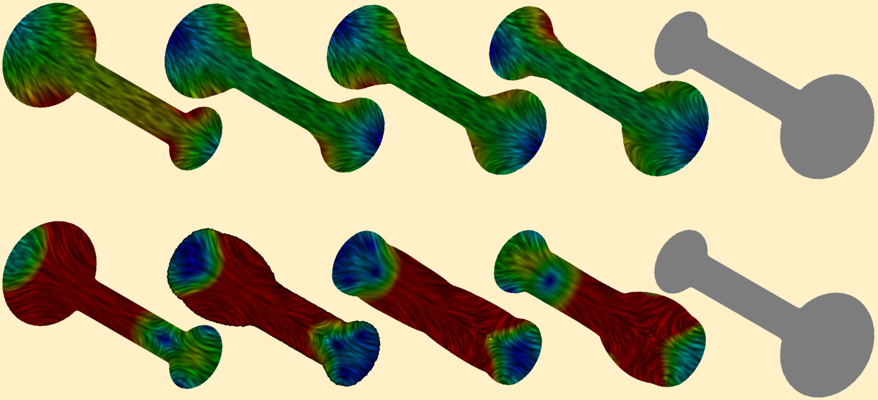

$\lambda/\mu = 100$

Impact of the surface area term

without surface area term:

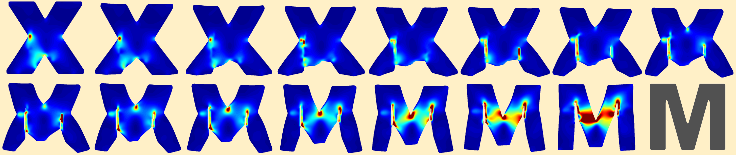

with surface area term:

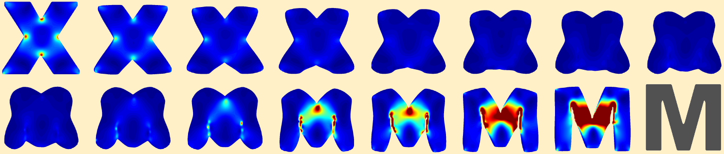

Complexity of shape space at a glance

U

M

C

Complexity of shape space at a glance

$S^1 \cdot \mathbf{U}$

$S^1 \cdot \mathbf{M}$

$S^1 \cdot \mathbf{C}$

Complexity of shape space at a glance

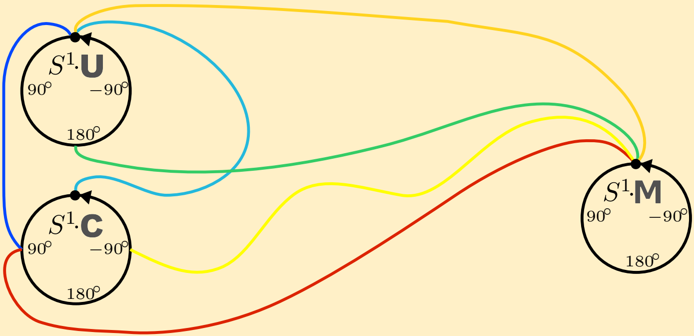

Complexity of shape space at a glance

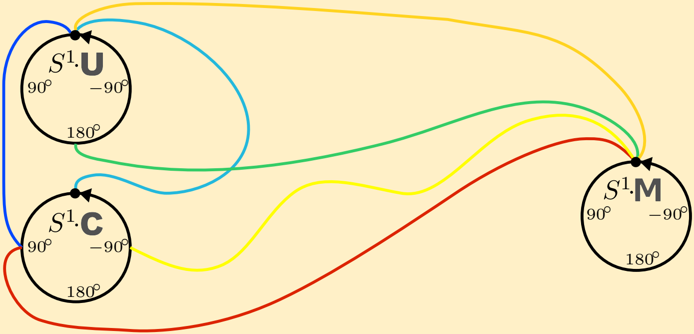

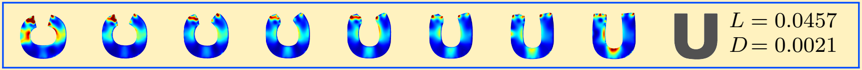

■ Complexity of shape space at a glance

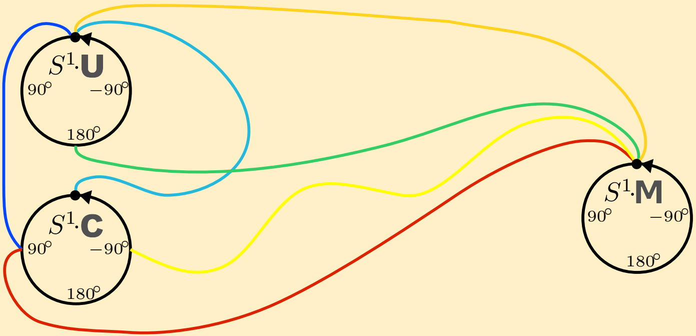

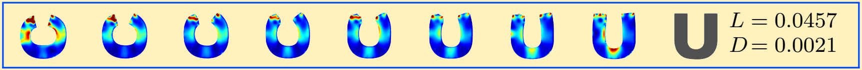

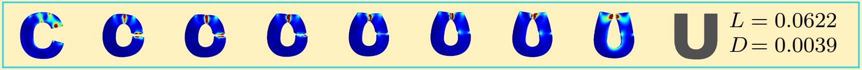

Complexity of shape space at a glance

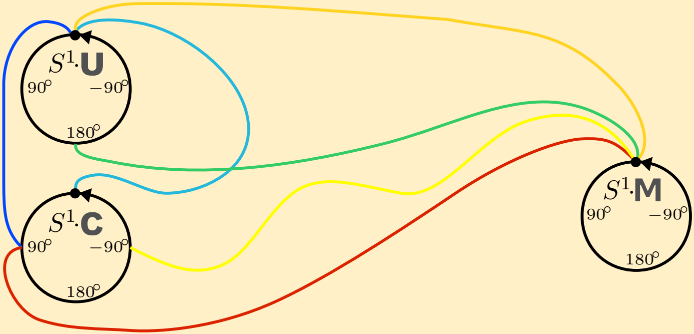

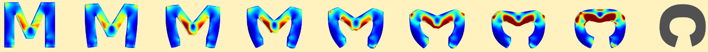

$L = 0.1040$
$D = 0.0108$

Complexity of shape space at a glance

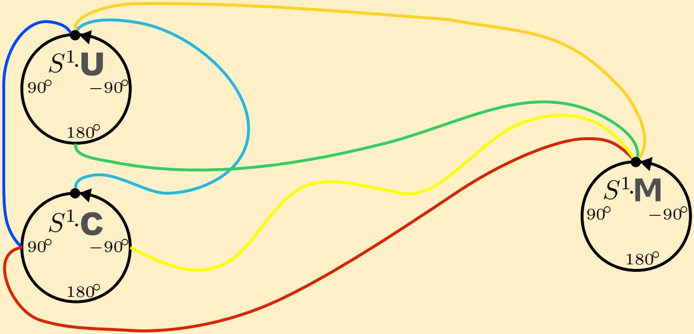

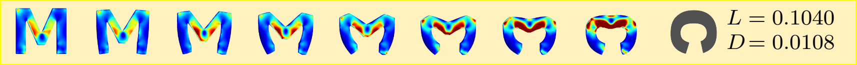

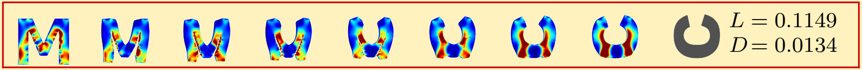

Complexity of shape space at a glance

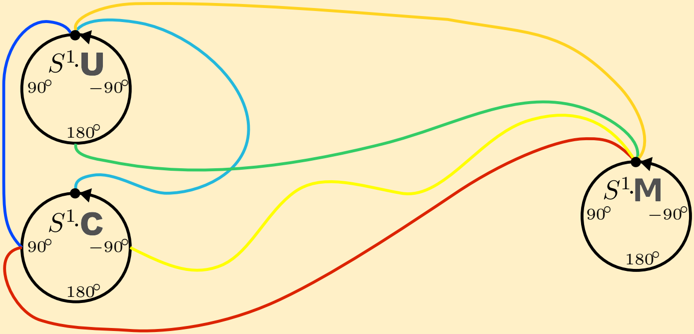

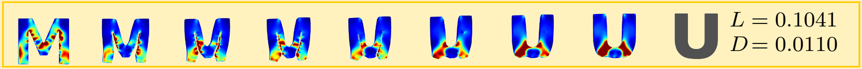

Complexity of shape space at a glance

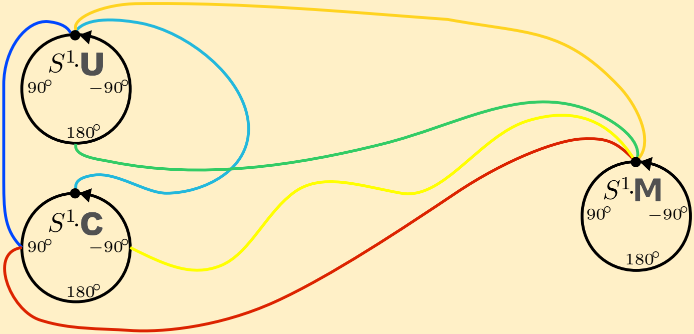

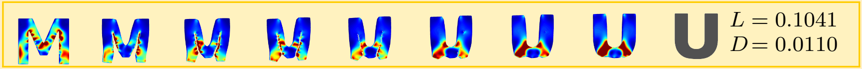

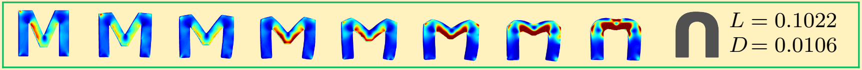

Geodesic between different 3D animals

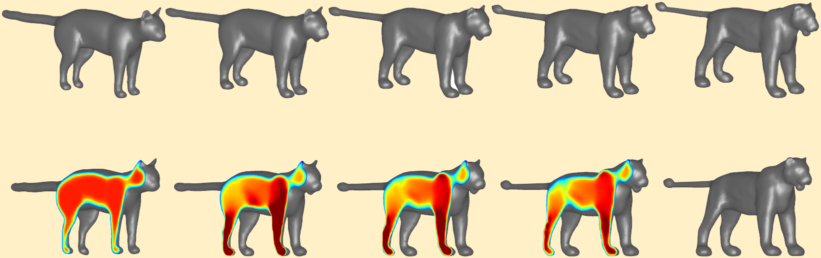

Geodesic between two 3D hand poses

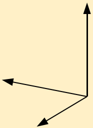

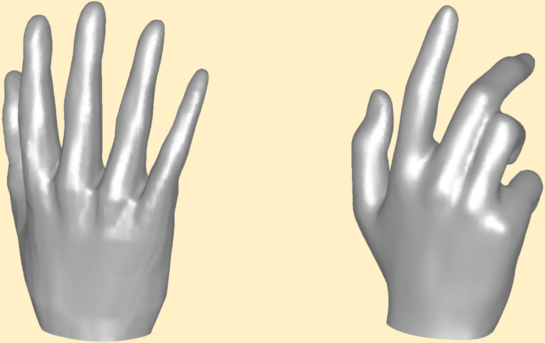

Geodesic between two 3D hand poses

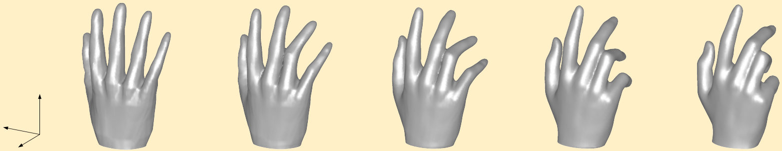

Geodesic between two 3D hand poses

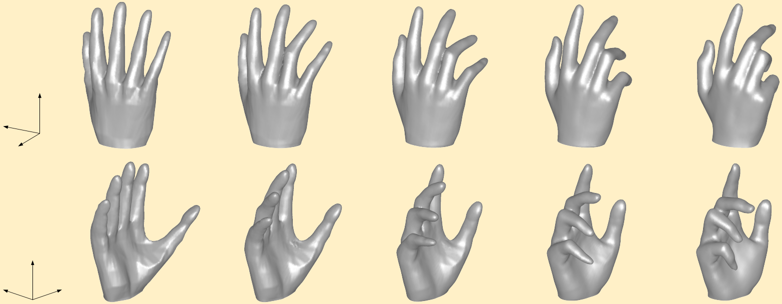

Geodesic between two 3D hand poses

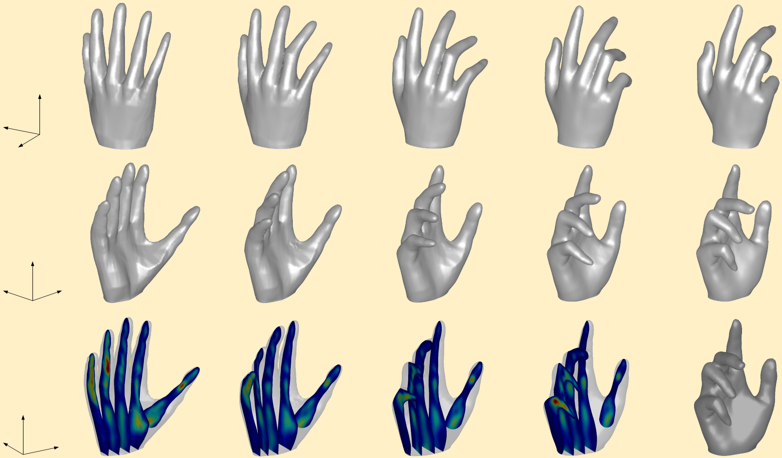

	B	B	B	X	X	M
B	-	3.8	12.1	25.9	24.7	37.7
B	-	-	10.1	25.5	24.4	37.7
B	-	-	-	23.5	23.6	32.3
X	-	-	-	-	13.6	31.2
X	-	-	-	-	-	40.4
M	-	-	-	-	-	-


	-	17.17	18.80	27.41	25.73	35.79
	-	-	12.70	21.48	24.55	34.98
	-	-	-	20.65	21.53	32.96
	-	-	-	-	17.30	22.14
	-	-	-	-	-	17.69
	-	-	-	-	-	-

left: geodesic distances between letter shapes.
right: geodesic distances between scanned 3D feet (data courtesy of adidas).

- Time discrete geodesic paths
- A relaxed formulation
- The numerical algorithm
- Limit of the time discrete model
- Qualitative properties of the model
- Generalized models

Geodesics in the presence of partial occlusion

Frequently, one would like to

- evaluate the distance of a partially occluded shape from a given template shape,
- restore partially occluded shapes based on some template shape.

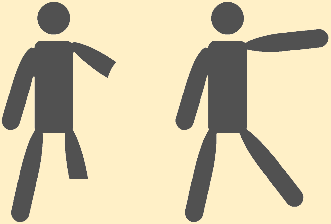

Let us suppose that the domain $\mathcal{O}_0$ associated with shape $\mathcal{S}_A = \partial\mathcal{O}_0$ is partically occluded. Then, replace the mismatch term $\mathcal{E}_{\text{match}}[\phi_1, \mathcal{S}_0, \mathcal{S}_1] = \mathrm{vol}(\mathcal{O}_0 \triangle \phi_1^{-1}(\mathcal{O}_1))$ by the term

$$\tilde{\mathcal{E}}_{\text{match}}[\phi_1, \mathcal{S}_0, \mathcal{S}_1] = \mathrm{vol}(\mathcal{O}_0 \setminus \phi_1^{-1}(\mathcal{O}_1))\,.$$

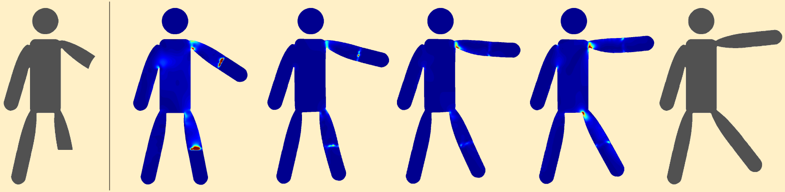

in the numerical implementation: insert a masking function $H_\varepsilon(\mathrm{Erosion}_\varepsilon[u_0])$ and obtain

$$\tilde{\mathcal{E}}^{\varepsilon}_{\text{match}}[\phi_1, u_0, u_1] = \int_\Omega \left(H_\varepsilon(u_1 \circ \phi_1) - H_\varepsilon(u_0)\right)^2 H_\varepsilon(\mathrm{Erosion}_\varepsilon[u_0])\,\mathrm{d}x\,.$$

to take advantage of adding parts to "loose" ends of $\mathcal{O}_0$.

Only taking into account shapes which are outer boundary contours $\mathcal{S} = \partial\mathcal{O}$ of open objects $\mathcal{O} \subset \mathbb{R}^d$ is rather limiting in some applications:

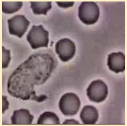


nonlinear interpolation between multi–component objects?

A geodesic between multi–component objects should match corresponding components, and a change in relative position of components naturally has to contribute to the geodesic path length.

Task: Compute a geodesic path

$$(\mathcal{S}^i(t))_{i=1,\dots,m} = (\partial\mathcal{O}^i(t))_{i=1,\dots,m}$$

with $t \in [0,1]$ between two multi–component shapes $(\mathcal{S}^i_A)_{i=1,\dots,m} = (\partial\mathcal{O}^i_A)_{i=1,\dots,m}$ and $(\mathcal{S}^i_B)_{i=1,\dots,m} = (\partial\mathcal{O}^i_B)_{i=1,\dots,m}$.

The geodesic path is supposed to be generated by a joint motion field $v(t) : \bigcup_{i=1,\ldots,m} \mathcal{O}^i(t) \to \mathbb{R}^d$ from $\bigcup_{i=1,\ldots,m} \mathcal{O}^i_A$ to $\bigcup_{i=1,\ldots,m} \mathcal{O}^i_B$.

The resulting total dissipation:

$$\mathbf{Diss}[v] = \int_0^1 \int_{\bigcup_{i=1,\ldots,m} \mathcal{O}^i(t)} \frac{\lambda}{2} (\mathrm{tr}\epsilon[v])^2 + \mu \,\mathrm{tr}(\epsilon[v]^2) \,\mathrm{d}x \,\mathrm{d}t \,.$$

with the flow constraint $v(x) \perp \nu[\mathcal{S}_i](x)$ for $x \in \mathcal{S}_i$.  

Modifications in the definition of a discrete geodesic:

$$\sum_{k=1}^K \mathcal{W}[\phi_k, (\mathcal{S}^i_{k-1})_{i=1,\ldots,m}] := \sum_{k=1}^K \int_{\bigcup_{i=1,\ldots,m} \mathcal{O}^i_{k-1}} W(\mathcal{D}\phi_k) \,\mathrm{d}x \,,$$

with $\phi_k(\mathcal{S}^i_{k-1}) = \mathcal{S}^i_k$ for $k = 1, \ldots, K$, $i = 1, \ldots, m$.

Generalized relaxed formulation:

$$\mathcal{E}^{\delta}_{\tau}[(\phi_k, (\mathcal{S}^i_{k-1})_{i=1,\dots,m}, (\mathcal{S}^i_k)_{i=1,\dots,m})_{k=1,\dots,K}]$$
$$= \sum_{i=1}^{K}\left(\frac{1}{\tau}\mathcal{E}^{\delta}_{\text{deform}}[\phi_k, (\mathcal{S}^i_{k-1})_{i=1,\dots,m}] + \sum_{i=1}^{n}\left(\eta\mathcal{E}_{\text{match}}[\phi_k, \mathcal{S}^i_{k-1}, \mathcal{S}^i_k] + \mu\tau\mathcal{E}_{\text{area}}[\mathcal{S}^i_k]\right)\right)$$

in the numerical implementation:

consider m level set functions to distinguish $n = 2^m$ different phases represented by objects $\mathcal{O}^i$, $i = 1, \dots, m$, as well as all possible combinations of overlapping [Chan Vese '01].

E.g. the problem   can is treated with $m = 2$ level set functions for $2^m = 4$ phases.

Single phase geodesic:

Multi–component geodesic:

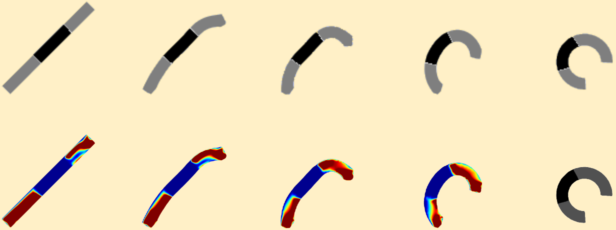

Nonlinear interpolation in multi–component cell motion

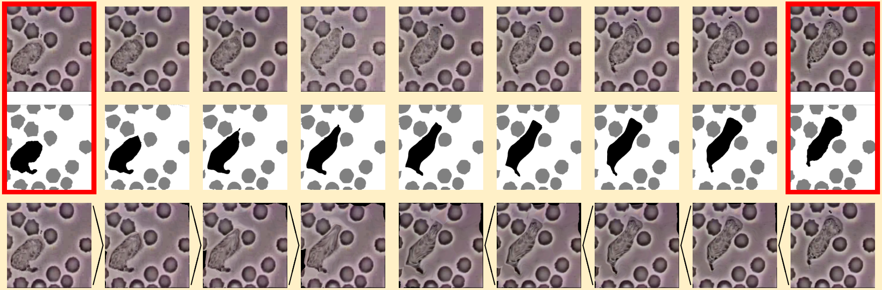

■ Nonlinear interpolation in case of human motion

Path based, Riemannian, viscous flow approach:

$$\mathbf{Diss}\left[(v(t),\mathcal{O}(t))_{t\in[0,1]}\right] + \gamma\mathcal{F} + \mu\mathcal{L} \to \min$$
with $\mathcal{O}(0) = \mathcal{O}_A\,,\ \mathcal{O}(1) = \mathcal{O}_B$

State based, non Riemannian, elastic approach:

$$\mathcal{W}[\mathcal{O}_A,\phi] \to \min \quad \text{with } \phi(\mathcal{O}_A) = \mathcal{O}_B$$

- choice depends on the applications and the underlying physics
- Path based approach requires the solution of a variational problem in $\mathbb{R}^{d+1}$, the state based approach a problem in $\mathbb{R}^d$.
- state based approach does not lead to a true distance:

  no triangle inequality: $d_{\text{elast}}(\mathcal{S}_A,\mathcal{S}_B) \leq d_{\text{elast}}(\mathcal{S}_A,\mathcal{S}_C) + d_{\text{elast}}(\mathcal{S}_C,\mathcal{S}_B)$
  lack of the symmetry: $d_{\text{elast}}(\mathcal{S}_A,\mathcal{S}_B) = d_{\text{elast}}(\mathcal{S}_B,\mathcal{S}_A)$

- Non-uniqueness:

  path based approach: shortest paths need not to be unique

  state based approach: due to multiple minimizers in elasticity

- Use in quantitative shape analysis:

  path based approach: cluster analysis via possible via pairwise distance computations

  state based approach: due to the lack of a triangle inequality comparison via the dissimilarity measure only between one fixed shape and a set of varying shapes (averaging, PCA)

- Existence of time continuous shortest paths in the viscous flow model?
- How to define a distance between true surfaces?
- Are topological transitions possible in a rigorous sense in the viscous flow model?
- How to define an elastic shape median?
- How to accelerate computations ?

Mémoli, F., Sapiro, G.:

A theoretical and computational framework for isometry invariant recognition of point cloud data.

Foundations of Computational Mathematics **5** (2005) 313–347

Kendall, D.G.:

Shape manifolds, procrustean metrics, and complex projective spaces.

Bull. London Math. Soc. **16** (1984) 81–121

Klassen, E., Srivastava, A., Mio, W., Joshi, S.H.:

Analysis of planar shapes using geodesic paths on shape spaces.

IEEE Transactions on Pattern Analysis and Machine Intelligence **26**(3) (2004) 372–383

Yezzi, A.J., Mennucci, A.:

Conformal metrics and true "gradient flows" for curves.

In: ICCV 2005: Proceedings of the 10th IEEE International Conference on Computer Vision. (2005) 913–919

Michor, P.W., Mumford, D., Shah, J., Younes, L.:

A metric on shape space with explicit geodesics.

Rend. Lincei Mat. Appl. (9) (2008) 25–57

Bibliography ≫

II

Kilian, M., Mitra, N.J., Pottmann, H.:

Geometric modeling in shape space.

In: ACM Transactions on Graphics. Volume 26. (2007) #64, 1–8

Fuchs, M., Jüttler, B., Scherzer, O., Yang, H.:

Shape metrics based on elastic deformations.

J. Math. Imaging Vis. **35**(1) (2009) 86–102

Rumpf, M., Wirth, B.:

A nonlinear elastic shape averaging approach.

SIAM Journal on Imaging Sciences **2**(3) (2009) 800–833

Wirth, B., Bar, L., Rumpf, M., Sapiro, G.:

A continuum mechanical approach to geodesics in shape space.

submitted to IJCV (2010)

Droske, M., Rumpf, M.:

Multi scale joint segmentation and registration of image morphology.

IEEE Transaction on Pattern Recognition and Machine Intelligence **29**(12) (2007) 2181–2194

Charpiat, G., Faugeras, O., Keriven, R.:

Approximations of shape metrics and application to shape warping and empirical shape statistics.

Foundations of Computational Mathematics **5**(1) (2005) 1–58

Bibliography ≫

III

Miller, M.I., Younes, L.:

Group actions, homeomorphisms, and matching: a general framework.

International Journal of Computer Vision **41**(1–2) (2001) 61–84

Michor, P.W., Mumford, D.:

Riemannian geometries on spaces of plane curves.

J. Eur. Math. Soc. **8** (2006) 1–48

Fletcher, P.T., Lu, C., Joshi, S.:

Statistics of shape via principal geodesic analysis on Lie groups.

In: IEEE Computer Society Conference on Computer Vision and Pattern Recognition CVPR. Volume 1. (2003) 95–101

Fletcher, T., Venkatasubramanian, S., Joshi, S.:

Robust statistics on Riemannian manifolds via the geometric median.

In: IEEE Conference on Computer Vision and Pattern Recognition (CVPR). (2008)

Berkels, B., Linkmann, G., Rumpf, M.:

An $SL(2)$ invariant shape median.

(2009) submitted.

Charpiat, G., Faugeras, O., Keriven, R., Maurel, P.:
Distance-based shape statistics.
In: Acoustics, Speech and Signal Processing, 2006 (ICASSP 2006). Volume 5. (2006)

Rumpf, M., Wirth, B.:
An elasticity approach to principal modes of shape variation.
In: Proceedings of the Second International Conference on Scale Space Methods and Variational Methods in Computer Vision (SSVM 2009). Volume 5567 of Lecture Notes in Computer Science. (2009) 709–720

Dambreville, S., Rathi, Y., Tannenbaum, A.:
A shape-based approach to robust image segmentation.
In Campilho, A., Kamel, M., eds.: IEEE Computer Society Conference on Computer Vision and Pattern Recognition. Volume 4141 of LNCS. (2006) 173–183

Bronstein, A., Bronstein, M., Kimmel, R.:
Numerical Geometry of Non-Rigid Shapes.
Monographs in Computer Science. Springer (2008)

Manay, S., Cremers, D., Hong, B.W., Yezzi, A.J., Soatto, S.:
Integral invariants for shape matching.
IEEE Transactions on Pattern Analysis and Machine Intelligence **28**(10) (2006) 1602–1618

Pennec, X., Stefanescu, R., Arsigny, V., Fillard, P., Ayache, N.:
Riemannian elasticity: A statistical regularization framework for non-linear registration.
In: Medical Image Computing and Computer-Assisted Intervention - MICCAI 2005. LNCS (2005) 943–950

Karcher, H.:
Riemannian center of mass and mollifier smoothing.
Communications on Pure and Applied Mathematics **30**(5) (1977) 509–541

Fletcher, P., Lu, C., Pizer, S., Joshi, S.:
Principal geodesic analysis for the study of nonlinear statistics of shape.
Medical Imaging, IEEE Transactions on **23**(8) (2004) 995–1005

Schmidt, F.R., Clausen, M., Cremers, D.:
Shape matching by variational computation of geodesics on a manifold.
In: Pattern Recognition. Volume 4174 of LNCS., Springer (2006) 142–151

Younes, L.:
Computable elastic distances between shapes.
SIAM J. Appl. Math **58**(2) (April 1998) 565–586

Delfour, M.C., Zolésio, J.:
Geometries and Shapes: Analysis, Differential Calculus and Optimization.
Adv. Des. Control 4. SIAM, Philadelphia (2001)

Zolésio, J.P.:
Shape topology by tube geodesic.
In: IFIP Conference on System Modeling and Optimization No 21,. (2004) 185–204

Dupuis, D., Grenander, U., Miller, M.:
Variational problems on flows of diffeomorphisms for image matching.
Quarterly of Applied Mathematics **56** (1998) 587–600

Beg, M.F., Miller, M.I., Trouvé, A., Younes, L.:
Computing large deformation metric mappings via geodesic flows of diffeomorphisms.
International Journal of Computer Vision **61**(2) (February 2005) 139–157

Glaunès, J., Qiu, A., Miller, M.I., Younes, L.:
Large deformation diffeomorphic metric curve mapping.
International Journal of Computer Vision **80**(3) (2008) 317–336

Wirth, B., Bar, L., Rumpf, M., Sapiro, G.:
Geodesics in shape space via variational time discretization.
In: Proceedings of the 7th International Conference on Energy Minimization Methods in Computer Vision and Pattern Recognition (EMMCVPR'09). Volume 5681 of LNCS. (2009) 288–302

Chorin, A.J., Marsden, J.E.:
A Mathematical Introduction to Fluid Mechanics. Volume 4 of Texts in Applied Mathematics.
Springer (1990)

Nečas, J., Šilhavý, M.:
Multipolar viscous fluids.
Quarterly of Applied Mathematics **49**(2) (1991) 247–265

Ciarlet, P.G.:
Three-dimensional elasticity.
Elsevier Science Publishers B. V. (1988)

Ball, J.:
Global invertibility of Sobolev functions and the interpenetration of matter.
Proceedings of the royal Society of Edinburgh **88A** (1981) 315–328

Chan, T.F., Vese, L.A.:
Active contours without edges.
IEEE Transactions on Image Processing **10**(2) (2001) 266–277

Bibliography ≫

VIII

Mumford, D., Shah, J.:

Optimal approximation by piecewise smooth functions and associated variational problems.

Communications on Pure Applied Mathematics **42** (1989) 577–685

Rumpf, M., Wirth, B.:

An elasticity-based covariance analysis of shapes.

International Journal of Computer Vision (2009) accepted.